230789

Geotechnical Slope Stability Evaluation
ASW System Bypass, Unit 1
Diablo Canyon Power Plant
San Luis Obispo County, California

Prepared for

Pacific Gas & Electric Company
245 Market Street, Room 823B N9B
San Francisco, California 94106

HLA Project No. 10183 ASWCALC

W. Andrew Herlache
Geotechnical Engineer

Robert Pyke, Ph.D.
Geotechnical Engineer

July 3, 1996

Harding Lawson Associates
150 Fourth Street, Suite 527
San Francisco, California 94103
(415) 543-8422

CONTENTS

PLATES

DISTRIBUTION

1.0 INTRODUCTION

This report presents the results of Harding Lawson Associates' (HLA's) geotechnical slope stability evaluation for the proposed Auxiliary Saltwater (ASW) System Bypass, Unit 1, at Diablo Canyon Power Plant in San Luis Obispo County, California. The purpose of our study was to evaluate the stability of the existing, approximately 50-foot-high slope in the vicinity of the proposed bypass and to develop conclusions regarding potential deformations of the slope during the design-level earthquake. HLA previously performed a field and laboratory investigation for the proposed bypass and presented the results in our report dated May 8, 1996.

Our services were provided in accordance with our proposal dated April 4, 1996, and Pacific Gas & Electric Company's (PG&E's) Contract Number Z78-1018-96 and Contract Work Authorization (CWA) 96-02 dated April 8, 1996. During the course of our work, our scope of services was modified to include evaluation of the liquefaction potential of fill materials southwest of the subject slope and to assess liquefaction-induced settlement and impacts on slope stability.

We obtained information regarding the project through meetings with PG&E on November 17 and December 18, 1995; by reviewing the project plans; and by reviewing several documents regarding existing conditions, construction procedures, and the proposed modifications. A complete list of the documents used in our evaluation is presented in Section 5.0, References.

The existing ASW piping system consists of two 24-inch-diameter pipelines, which are located above a shelf that is attached to the Circulating Water Intake (CWI) conduits. The existing pipes are steel and have experienced some corrosion. The new project consists of bypassing the potential zone of corrosion with new piping.

The ASW bypass zone extends to the northeast approximately 400 feet from the existing Intake Structure, as shown on Plate 1. The ground surface in this area varies from approximately Elevation 18 feet[1] near the Intake Structure to Elevation 75 feet near the top of an existing 2:1 (horizontal to vertical) slope that is approximately 50 feet high.

The ASW bypass will consist of two new 24-inch-diameter pipes located in the existing backfill adjacent to and above the CWI conduits. The backfill generally consists of native material excavated from elsewhere onsite. The bottoms of the new pipes will be located approximately 5 to 10 feet below the existing ground surface. The pipes will not be connected to the CWI conduits, except at the north end. The new pipes will traverse the slope mentioned above.

The scope of our geotechnical services was to evaluate the slope stability by performing the following analyses:

- Static stability analyses using the computer program UTEXAS3 (Wright, 1991), which incorporates standard limit equilibrium methods to evaluate the static factor of safety of the slope
- Pseudostatic analyses using the computer program UTEXAS3 to determine the yield accelerations for potential failure surfaces analyzed during the static analyses
- If necessary, Newmark deformation analyses using the computer program TNMN (TAGA, 1996) to help evaluate potential deformations of the slope using earthquake acceleration time histories provided by PG&E

On the basis of the results of our analyses, we were to develop conclusions and recommendations regarding the following:

---

[1] Mean sea level (MSL).

- The static stability of the slope
- The potential for slope failure during the design earthquake ground motions
- The magnitude of anticipated slope deformations during the design earthquake, the uncertainty associated with this estimate, and the likely earth forces on the ASW piping resulting from these movements
- Backfilling requirements for the ASW piping to minimize deformations of the slope and piping system, if appropriate

As previously mentioned, our scope was expanded to include performing an evaluation of the liquefaction potential of fill soils located southwest of the subject slope and to provide conclusions regarding the impact of liquefaction on ground surface settlements and slope stability.

In performing our evaluation, HLA was assisted by Dr. Robert Pyke, Consulting Engineer, of Lafayette, California.

2.0 SITE AND SUBSURFACE CONDITIONS

Information regarding the site and subsurface conditions is presented in our May 8, 1996 report. Following is a summary of the surface conditions, the existing structures below grade, the subsurface conditions, the site seismicity, and the engineering properties used in our analyses.

2.1 Surface Conditions

Ground surface elevations at the ASW bypass site range from about 18 to 75 feet. The ground surface is approximately Elevation 18 feet around the Intake Structure, Control Building, and Intake Access Control Office and Storage Building; Elevation 24 feet on the access drive northeast of the Office and Storage Building; Elevation 24 feet at the toe of the slope northeast of the Intake Structure; and Elevation 75 feet at the top of the slope. The ground surface surrounding the three structures and along the access road is paved and generally level. The slope behind the access road is moderately vegetated.

2.2 Existing Structures Below Grade

The buried portions of the existing ASW piping and CWI conduits are approximately 1,600 feet long, extending from the Intake Structure to the Turbine Generator Building. The northernmost portion of the CWI conduit foundations are bottomed between Elevations 50 and 55 feet. The conduits descend at a 67 percent grade from Elevation 50 feet, near the top of the slope, to Elevation -20 feet, near the toe of the slope, and then extend horizontally to the Intake Structure. Plate 2 presents a cross section of the slope and CWI conduits at the location shown on Plate 1. The CWI conduits and Intake Structure foundations are all bottomed on rock.

2.3 Subsurface Conditions

As previously mentioned, the ASW bypass pipelines will be placed in the existing backfill for the CWI conduits, as shown on Plates 1 and 2. On the basis of our test borings, our review of previous investigations, and our review of construction drawings, we estimate that the backfill along the ASW bypass alignment is as thick as approximately 40 feet and is underlain by moderately strong rock consisting of shale, sandstone, and possibly tuff. The sides of the excavations to construct the CWI conduits and the Intake Structure were sloped near the ground surface and near vertical for the lower portions of the excavations. Therefore, the depth of the existing backfill adjacent to these structures is somewhat less than the depth of the CWI foundations. The backfill thickness decreases with distance from the structure.

The maximum backfill thickness in the area of the proposed ASW bypass alignment is estimated to be approximately 10 to 35 feet along the section of bypass extending down the 2:1 slope; 35 to 40 feet along the section of bypass extending from the base of the slope (Boring B-1) to a point near Boring B-4; 6 to 8 feet along the section of bypass extending between Conduits 1-2 and 2-1 (Boring B-2); and 25 to 30 feet along the section of bypass extending south of Conduit 2-2 (Boring B-3).

The backfill material generally consists of the following three main material types:

1. A mixture of varying quantities of angular gravel, sand, and clay that is predominantly from onsite sources of native soil and rock
2. Granular import material
3. Poorly graded sand that appears to be imported pipe bedding material

The locations and engineering properties of each backfill material are discussed in more detail in the following sections, as are the underlying rock and the groundwater conditions.

2.3.1 Backfill from Onsite Sources (Cohesive Fill)

Backfill from onsite sources consists of a mixture of varying quantities of angular gravel, sand, and clay. Backfill from onsite sources was used predominantly around and above the CWI conduits. These gravels, sands, and clays were the predominant material encountered in our test pits and represent approximately 70 percent of the material encountered in our test borings. Backfill from onsite sources was encountered to a depth of 20 feet in Boring B-1, 6 feet in Boring B-2, 14 feet in Boring B-3, and 18 feet in Boring B-4. These materials are believed to represent a mixture of native soil and rock that was excavated from onsite sources.

The percentage of each primary particle size range was found to vary, which could be explained by variation in soil cover thickness at the original borrow source.

Laboratory tests indicated that the material has the following properties:

- Maximum particle size, 2 inches
- Percent gravel, 8 to 48
- Percent sand, 20 to 44
- Percent fines, 11 to 66
- Dry density, 92 to 124 pounds per cubic foot (pcf)
- Moisture content, 7.8 to 28.0 percent
- Plasticity index 17 to 21; liquid limit 38 to 45

Compaction curves tests were performed on bulk samples obtained from Test Boring B-1 and Test Pits TP-1 and TP-3. The results indicate that the maximum dry density is affected by the percentage of gravel and fines present in the sample. Our laboratory tests indicate that the percentage of gravel and fines in the backfill material varies considerably. Therefore, because of the limited number of compaction tests, we were not able to quantitatively determine the percent of relative compaction at all locations where in situ densities were measured. On the basis of our evaluation of the laboratory data and visual observation of the backfill in the test pits, we conclude that the backfill relative compaction generally ranges from approximately 85 to 95 percent[2].

Because the backfill contains significant amounts of clayey fines, we believe, it will behave as a cohesive material. For our analyses, we selected undrained shear strength and total unit weight parameters to model the backfill from onsite sources. On the basis of published literature regarding the undrained strength of compacted fill (Duncan et al., 1980), we conservatively selected a design undrained shear strength of 2,500 pounds per square foot (psf) to model the cohesive fill. We used a total unit weight of 125 pcf for the cohesive fill in our analyses.

These assumed properties are confirmed by the results of laboratory tests on both relatively undisturbed and remolded samples of the backfill from onsite sources. The results of the TxUU shear strength tests on relatively undisturbed samples indicate that the undrained shear strength ranged from 910 to 3,360 psf. The lower strengths are believed to be a result of sample disturbance due to gravel-sized particles. Excluding the low values, the average strength from the relatively undisturbed samples tested is approximately 2,960 psf. In addition to shear strength tests performed on undisturbed samples collected in the field, TxUU tests were performed on three remolded samples. TxUU shear strength test results indicate that the

[2] Relative compaction refers to the in-place dry density of soil expressed as a percentage of the maximum dry density of the same material, as determined by the ASTM D1557 laboratory compaction procedure.

undrained shear strength ranged from 4,250 psf to 6,600 psf for cell pressures of 500 psf to 3,000 psf. The average of these tests is approximately 5,420 psf. All of the remolded tests were conducted at a dry density, moisture content, and total unit weight of approximately 104 pcf, 15.5 percent, and 120 pcf, respectively. The average of the TxUU tests on the relatively undisturbed and remolded samples indicates that the use of 2,500 psf in our calculations is very conservative.

2.3.2 Granular Import Backfill (Granular Fill)

Granular import backfill was encountered in several borings. Poorly graded gravel with clay and sand was encountered in Boring B-3 at depths of 14 to 25 feet; poorly graded sand with gravel and poorly graded sandy gravel was encountered in Boring B-4 at depths of 18 to 31-1/2 feet; and clayey sand with gravel was encountered in Boring B-1 at depths of 20 to 22-1/2 feet. Blow counts ranged from 15 blows per foot to 35 blows for 2 inches, with an average of approximately 100 blows per foot, indicating that the granular backfill is generally very dense. Boring B-4 encountered a poorly graded sand with gravel at a depth of 25 feet (Elevation -1 foot) that had a blow count of 15 blows per foot, indicating that it is medium dense. This medium dense material is believed to be fill that was placed during the repair of electrical conduits in the early 1980s. This material was reportedly jetted to achieve compaction. On the basis of the variation in blow counts for the granular import backfill and the method of compaction used, we judge that the lower density zones are confined to localized areas of the fill.

Laboratory tests indicated that the poorly graded gravel with clay has the following soil properties:

- Percent gravel, 45
- Percent sand, 44
- Percent fines, 11
- Dry density, 115 pcf
- Moisture content, 8.8 percent

Laboratory tests also indicated that the clayey sand with gravel has the following soil properties:

- Percent fines, 17
- Dry density, 120 to 121 pcf
- Moisture content, 6.9 to 7.1 percent

To model most of the granular fill for our analyses, we conservatively assumed a friction angle of 34 degrees, a cohesion of zero, and a total unit weight of 120 pcf on the basis of published literature (Hunt, 1984) and the observed blow counts. As discussed in a subsequent section of this report, the medium dense sand encountered at a depth of 25 feet is believed to be potentially liquefiable. To account for this in our analyses, we assumed that this material would develop positive pore water pressures during the design level earthquake. This potential pore water pressure increase would reduce the sand's effective strength. To model this, we assigned the sand from Elevation 0 to -5 feet a residual strength of 700 psf based on the correlations presented by Seed and Harder, 1990.

2.3.3 Poorly Graded Sand Import Bedding Material (Granular Bedding)

Poorly graded sand was encountered in Boring B-1 at depths of 22.5 to 26.5 feet. This is the material believed to bed the existing ASW pipelines. The sand was encountered 4 to 5 feet higher than and several feet south of the existing ASW backfill envelope. This may be partly the result of rock overbreak in the excavations, as seen in historic photos, to comply with project specifications that all fill placed below Elevation 6 feet should be granular, or the result of work performed to repair electrical ducts in the early 1980s. This material had a blow count of 18 at a depth of 25 feet (Elevation -1 foot), indicating

that it is medium dense at that location. The project specifications required that this material (bedding sand for piping and conduit envelopes) be compacted to at least 95 percent relative compaction.

In our analyses, we used a vertical cross section aligned with the main axis of the backfilled trench for the existing ASW piping. In modeling the existing bedding sand, we increased the strength parameters to account for the fact that the sand was confined on one side by the existing CWI conduits and on the other side by the rock face that was cut to install the CWI conduits and the existing ASW piping. Assuming that the existing bedding sand is medium dense to dense, we estimated a friction angle of 34 degrees (Hunt, 1984) for triaxial loading conditions. Mitchell (1993) indicated that the friction angle in plane strain is typically 10 percent larger than that measured in triaxial compression because the constraint against lateral deformation causes an increase in the effective confining pressure. Therefore, we increased the friction angle to 37.4 degrees to better model the plane strain field conditions. Then, because an assumed failure zone must shear the sides of the sand envelope in addition to a horizontal shear plane, we further increased the effective friction angle, accounting for the field geometry and assuming at-rest conditions.

This factor was computed by setting the effective friction angle equal to:

$$\phi_{effective} = \tan^{-1} [(1+K_o) \tan \phi]$$

where $K_o = 1 - \sin \phi$

and where ϕ equals 37.4 degrees, K_o is 0.39, and $\phi_{effective}$ equals 47 degrees.

Therefore, to account for the effects of plane strain and the three-dimensional nature of the problem, we used a design friction angle of 47 degrees, a cohesion of zero, and a total unit weight of 120 pcf to model the existing bedding sand.

The sand encountered at Elevation -1 feet in Boring B-1 (above the existing ASW pipelines) had a blow count that is similar to that for the material encountered in Boring B-4 at that elevation. Because the sand is medium dense and below MSL, it is also considered potentially liquefiable. Therefore, we assumed that this material has the same properties as the granular import backfill located between Elevations 0 and -5 feet as discussed in Section 2.3.2.

2.3.4 Rock

The backfill materials and the CWI conduits are underlain by moderately strong rock consisting of shale, sandstone, and possible tuff. For the stability analyses, we conservatively assumed that the rock has the following properties: a friction angle of 30 degrees, a cohesion of 3,000 psf, and a unit weight of 140 pcf. These values are from previous HLA reports regarding Diablo Canyon Power Plant (HLA, 1978 and HLA, no date).

2.3.5 Groundwater Conditions

Only Boring B-4 encountered groundwater during our investigation. The water level measured was at a depth of 24 feet (approximately Elevation 0). As the site is immediately adjacent to the ocean, it is reasonable that the average groundwater level would be near MSL. Some seasonal and tidal fluctuation in the groundwater level likely occurs. For purposes of our analyses, we assumed a groundwater level of Elevation +3 feet.

2.4 Seismicity

The site is in a seismically active area of California and will likely experience strong ground shaking during the design life of the facility. Several previous studies have evaluated the site seismicity. PG&E provided HLA the design earthquake ground motions for use in our study. Five horizontal acceleration time histories were used in our study, and they include:

- The Hosgri (Newmark) ground motion
- The modified Pacoima Dam longitudinal ground motion
- The modified Pacoima Dam transverse ground motion
- The modified Tabas longitudinal ground motion
- The modified Tabas transverse ground motion

The Pacoima Dam and Tabas motions were modified as part of the Long-Term Seismic Program (LTSP) for the power plant. The peak ground acceleration (PGA) for the Hosgri time history is 0.75 gravity (g). The PGAs for the other records are 0.83 g.

For the purposes of this evaluation, it was assumed that the bedrock time histories and peak accelerations would apply directly to any potential sliding masses. We believe that more detailed analyses would likely show this assumption to be conservative, because the response of the backfill over the CWI conduits would vary from point to point and the average driving accelerations acting on a potential sliding mass would be less than the accelerations of the surrounding rock.

3.0 GEOTECHNICAL ANALYSES

3.1 General

This section describes the geotechnical engineering analyses performed for this study. The discussion includes a description of the methods and assumptions used. HLA performed the following analyses:

- Liquefaction potential and seismically induced settlement
- Static slope stability
- Pseudostatic slope stability

The geotechnical engineering properties used in our analyses are described in Section 2.0.

3.2 Liquefaction Potential

Soil liquefaction is a phenomenon in which saturated (submerged), cohensionless soils experience a temporary loss of strength because of the buildup of excess pore water pressure, especially during cyclic loadings, such as those induced by earthquakes. Soils most susceptible to liquefaction are loose, clean, saturated, uniformly graded, fine-grained sands.

Borings B-1 and B-4 encountered medium dense sands at a depth of 25 feet (Elevation -1 feet). These sands are believed to be a portion of the granular import backfill that was placed during original construction of the CWI conduits between the Intake Structure and the toe of the subject slope. As discussed in Section 2.0, only two of the blow counts in the granular import backfill would result in the classification of medium dense, while several others indicate that the granular backfill is very dense.

The granular backfill that is very dense or contains a significant amount of clayey fines is considered to be not susceptible to liquefaction. The zone of the medium dense sands that are located below the water table is believed to be confined to an area that is immediately southeast of the Unit 1 CWI conduits and approximately 10 to 20 feet wide and 100 feet long, as shown in HLA's June 25, 1996 letter report (HLA, 1996b). Based on the recent Boring B-4, we have assumed that this zone is 5 feet thick, from Elevation 0 to -5 feet. This is a conservative assumption, given that the fill was reportedly compacted to at least 95 percent relative compaction. It is more likely that the sands range from being medium dense to dense within the zone defined above.

We evaluated the potential for liquefaction using the procedures developed by Seed et al. (1985). In our analyses, we used a PGA of 0.83 g (HLA, 1996b). Our analyses indicate that there is a high probability of liquefaction for the medium dense sands located below the water table. As discussed in Section 2.0, we assigned a reduced strength to a zone that could liquefy during the design level earthquake, in accordance with the methods outlined in Seed and Harder (1990). In performing our analyses, we assumed that a 5-foot-thick layer from Elevation 0 to Elevation -5 feet could liquefy during an earthquake. This layer was assigned an undrained shear strength of 700 psf based on corrected blow counts in the range of 15 to 19 blows per foot. This is believed to be a conservative assumption, as the medium dense sand is located in a confined zone and is not a continuous layer throughout the lower portion of the site.

3.3 Static Slope Stability Analyses

3.3.1 Methodology and Assumptions

In performing our static slope stability analyses, we used the commercially available computer program UTEXAS3 (Wright, 1991). UTEXAS3 analyzes slope stability with circular and noncircular slip surfaces using limit-equilibrium methods. We analyzed both the circular and

noncircular slip surface, using Spencer's procedure (Spencer, 1967; Wright, 1969).

We analyzed potential failure surfaces that were perpendicular to the main axis of the ASW bypass. The location of the cross section used in our analyses is shown on Plate 1. We judge other potential failure surfaces and cross-section orientations to be noncritical, as the failure surfaces would be largely in rock.

Our analyses were performed using the cross-section data presented on Plate 2. The soil and rock properties used in the analyses are those presented in Section 2.0 and shown on Plate 2. The water table was assumed to be at Elevation +3 feet.

Our methodology included searching for circular and noncircular slip surfaces to obtain the potential failure surface with the lowest factor of safety. We evaluated potential slip surfaces along the upper portion of the slope, surfaces that exited near the toe of the slope, and deep surfaces that penetrated the potentially liquefiable layer. The search was continued until the critical slip surface was identified (the surface with the lowest computed factor of safety).

3.3.2 Results

The results of our static slope stability analyses are presented on Plate 3. The most critical potential slope surface was identified as a circular surface that passed through the toe of the slope, with a factor of safety of 3.24. Noncircular slip surfaces were also checked; generally, as the number of points defining the noncircular surface increased, the factor of safety decreased, and the surface approached that of a circular shape.

To check the factor of safety for a potential slip surface occurring in the upper portion of the slope, we limited the search to surfaces above Elevation 55 feet. For this case, we found that a circular slip surface tangent to Elevation 55 feet yielded the lowest factor of safety, 6.05.

We also checked the factor of safety for the potential slip surface that passed through the potentially liquefiable layer below the toe of the slope. In this case, the most critical slip surface had a noncircular shape and a factor of safety of 3.66. The noncircular shape was favored because of the relative weakness of the liquefiable layer; however, the factor of safety for this surface was greater than that for the toe circle previously identified.

We also considered a potential failure surface that passes along the interface of the proposed pipelines and the sand bedding material. While the interface friction between the steel pipeline and the sand will be relatively low, a failure surface would have to be a relatively narrow, three-dimensional surface for the interface friction to have a significant influence. If this were the case, the potential failure surface would also have to pass through the relatively strong cohesive fill between the pipeline and the ground surface. Because of the three-dimensional effect and the presence of the relatively strong cohesive fill, we judge that a failure through the pipeline/soil interface is not critical.

3.4 Pseudostatic Slope Stability Analyses

Pseudostatic analyses were performed to determine the yield acceleration for the critical slip surface obtained from the static slope stability analyses. The yield acceleration is defined as the horizontal acceleration coefficient that reduces the factor of safety to 1.0. Using the computer program UTEXAS3 and the strength parameters presented in Section 2.0, we varied the horizontal acceleration coefficients to identify the yield acceleration.

The results of our analyses indicate that the yield coefficient for the critical toe circular surface identified during the static stability analyses (static factor of 3.24) is 0.67 g.

3.5 Deformation Analysis

In view of the very high computed yield acceleration and the fact that very few peaks on the acceleration time histories exceed the yield acceleration, we did not perform a Newmark type analysis. The Newmark analysis was originally developed for evaluating relatively large deformation of dams and earth embankments during seismic events. These deformation were generally on the order of feet. Because of the simplifying assumptions used in the analyses, the Newmark methods are not appropriate for evaluating the very small deformations that would be expected for the slope under consideration. The very high yield acceleration implies that the slope will be essentially stable during a seismic event and that permanent deformations will be negligible.

4.0 CONCLUSIONS AND RECOMMENDATIONS

4.1 Liquefaction Potential and Seismically Induced Settlement

As discussed in Section 3.2, localized areas of the medium dense sand below the toe of the slope may liquefy during the design level earthquake. The effects of liquefaction will include reducing the strength of the sands during the event and potentially causing settlement of the ground surface following the event. Potential settlements are discussed in HLA, 1996b. We judge that no appreciable lateral movement will occur because of liquefaction.

4.2 Static Slope Stability

The analysis presented in Section 3.3 of this report indicates that the slope is and will remain stable under static loads. The most critical potential failure surface passes through the toe of the slope and has a factor of safety of approximately 3.2. This factor of safety is well above 1.5, which is generally accepted for design in California practice. Therefore, we judge that the slope will be stable under static loading conditions after the proposed ASW bypass system is installed.

4.3 Seismic Slope Stability

The analysis presented in Section 3.4 of this report indicates that the minimum yield acceleration is relatively high, at a value of 0.67 g. The PGAs for the design level earthquake are 0.75 g for the Hosgri event and 0.83 g for the Pacoima and Tabas events. Because the design time histories have very few peaks that exceed the 0.67 g yield acceleration, we judge that any permanent deformations of the slope during a seismic event will be very small. We judge that this conclusion also applies to an event that is 40 percent larger than the Pacoima and Tabas events (i.e., those with PGAs of 1.16 g), since any increase in the peak accelerations would likely result from high-frequency motion, which would not significantly impact accumulation of displacements.

Therefore, we conclude that the slope will be stable during a seismic event and that additional loads resulting from permanent deformation of the slope will not apply to the new ASW bypass pipes.

4.4 Pipe Backfill

On the basis of the results of the analyses, we judge that no special backfilling procedures will be required to isolate the pipes from anticipated slope deformation. Therefore, we recommend that as a minimum, the pipes be bedded in clean sands and that the sand extend to at least 12 inches above the tops of the pipes. The bedding and initial backfill sand should be compacted to at least 95 percent relative compaction. Trench backfill above the sand can consist of existing materials excavated to install the pipes. These materials should be moisture-conditioned to near optimum content, placed in lifts not exceeding 8 inches in loose thickness, and compacted to at least 90 percent relative compaction.

5.0 REFERENCES

Harding Lawson Associates, 1978. *Geotechnical Studies, Intake Structure, Water Storage Tanks, Diesel Fuel Oil Storage Tanks, Diablo Canyon Nuclear Power Plant, San Luis Obispo County, California*, April 12.

Harding Lawson Associates, No Date. *A Comprehensive Design Review of the Auxiliary Saltwater Piping System, Diablo Canyon Nuclear Power Plant, San Luis Obispo County, California.*

Harding Lawson Associates, 1996a. *Geotechnical Field and Laboratory Investigation, ASW System Bypass, Units 1 & 2, Diablo Canyon Power Plant, San Luis Obispo County, California*, May 8.

Harding Lawson Associates, 1996b. *Liquefaction Elevation, Proposed ASW Bypass, Diablo Canyon Power Plan, San Luis Obispo County, California*, June 25.

Hunt, Roy E., 1984. *Geotechnical Engineering Investigation Manual*. McGraw-Hill, Inc.

Mitchell, James K., 1993. *Fundamentals of Soil Behavior, Second Edition*, University of California, Berkeley. John Wiley & Sons, Inc.

Pacific Gas & Electric Company, 1986. *Specification for Construction of Intake Structure for Circulating Water System for Units 1 and 2, Diablo Canyon Site*, January 17.

Seed, H. B., K. Tokimatsu, L. F. Harder, and R. M. Chung, 1985. Influence of SPT procedures and liquefaction resistance evaluations, American Society of Civil Engineers, *Journal of Geotechnical Engineering*, Volume 111, No. 12, December.

Seed, Raymond B. and Leslie F. Harder, Jr., 1990. SPT-based analysis of cyclic pore pressure generation and undrained residual strength. 1990. *Volume 2, Memorial Symposium, Proceedings*, May. Ed. J. Michael Duncan. BiTech Publishers Ltd., Vancouver, B.C., Canada, p. 351.

Spencer, E. 1967. A method of analysis of the stability of embankments assuming parallel inter-slice forces, *Geotechnique*, Volume 17, No. 1, March, pp 11-26.

TAGA Engineering Systems and Software, 1996. *TNMN Users Guide*, Lafayette, California.

Tokimatsu, K. and H. B. Seed, 1987. Evaluation of settlement of sands due to earthquake shaking, American Society of Civil Engineers, *Journal of Geotechnical Engineering*, Volume 113, No. 8, August.

Wright, Stephen G., 1969. A study of slope stability and the undrained shear strength of clay shales. Thesis presented to the University of California, at Berkeley, California in partial fulfillment of the requirements for the degree of Doctor of Philosophy.

Wright, Stephen G., 1990. UTEXAS3, *A Computer Program for Slope Stability Calculations*, Shinoak Software, Austin, Texas, May 1990, Revised July 1991, September 1991.

Drawings

Pacific Gas & Electric Company, *Diablo Canyon Power Plant, Auxiliary Saltwater System Bypass Piping (Phase II) Units 1 & 2.*

- DWG SK-C-ASWB, Revision H, Sheet 4 of 4, Latest Revision Dated 10/09/95
- DWG SK-C-ASWB, Revision H, Sheet 1 of 3, Latest Revision Dated 09/13/95

Pacific Gas & Electric Company, *Profile of Intake Conduit 1-2, Circulating Water System, Diablo Canyon.*

- DWG 438097, Revision 8, Sheet 2 of 2 (Date Illegible)

PLATES

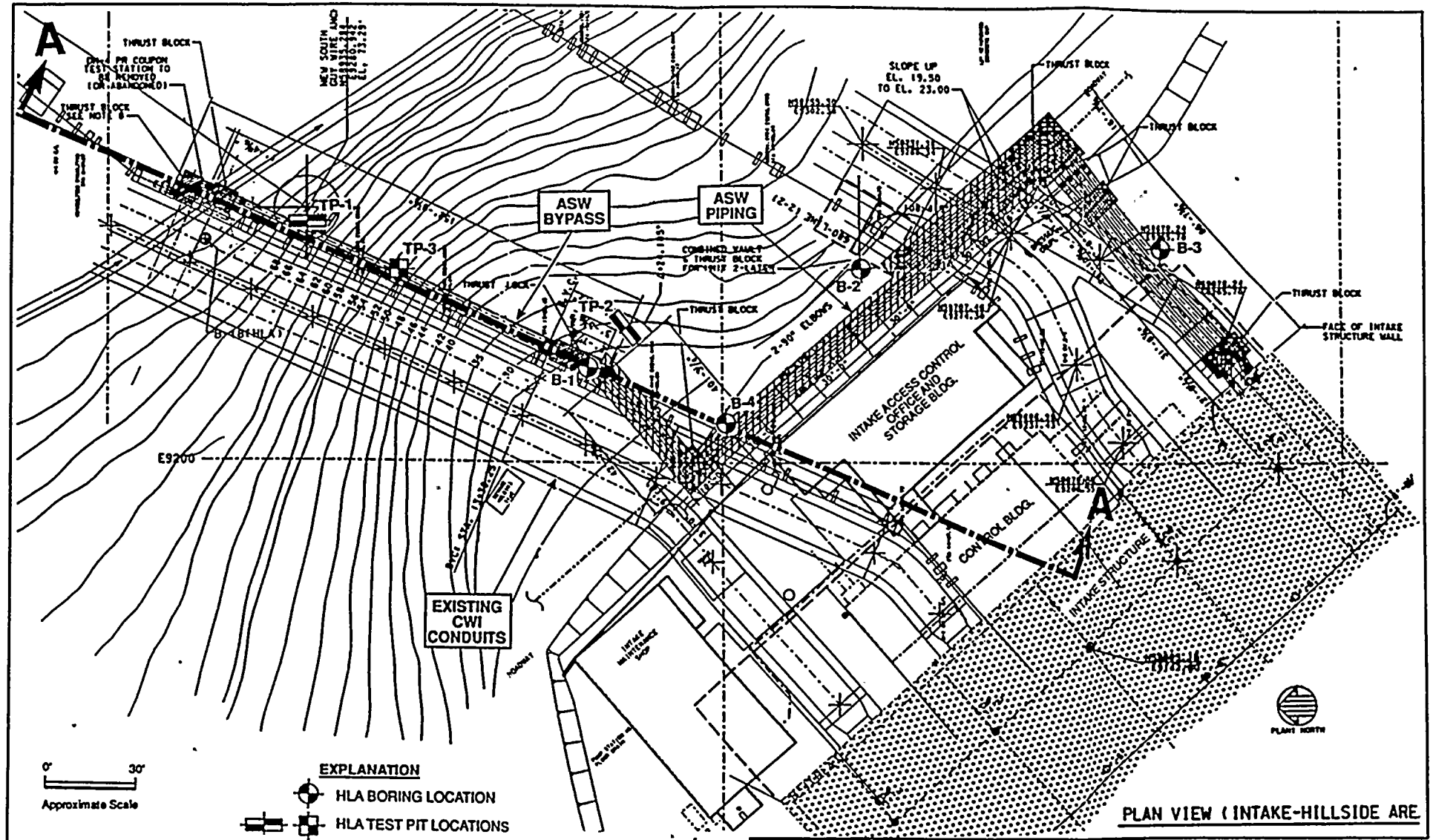

REFERENCE: Diablo Canyon Power Plant, Auxiliary Saltwater System, Bypass Piping Unit 1 & 2, Pacific Gas & Electric Company, San Francisco, California, dated September 13, 1995

PLAN VIEW (INTAKE-HILLSIDE ARE

Harding Lawson Associates
Engineering and Environmental Services

Site Plan
Diablo Canyon ASW Bypass
San Luis Obispo County, California

PLATE 1

DRAWN	JOB NUMBER	APPROVED	DATE	REVISED DATE
JMV	10183.ASW-CALC		5/96	

MATERIAL TYPE	DESCRIPTION	COHESION (PSF)	FRICTION ANGLE (DEGREES)	TOTAL UNIT WEIGHT (PCF)
1	FOUNDATION ROCK AND CONCRETE	3000	30	140
2	GRANULAR BEDDING	0	47	120
3	DENSE GRANULAR FILL BELOW WATER	0	34	120
4	MEDIUM DENSE GRANULAR FILL BELOW WATER	700	0	120
5	GRANULAR FILL ABOVE WATER	0	34	120
6	COHESIVE FILL	2500	0	125

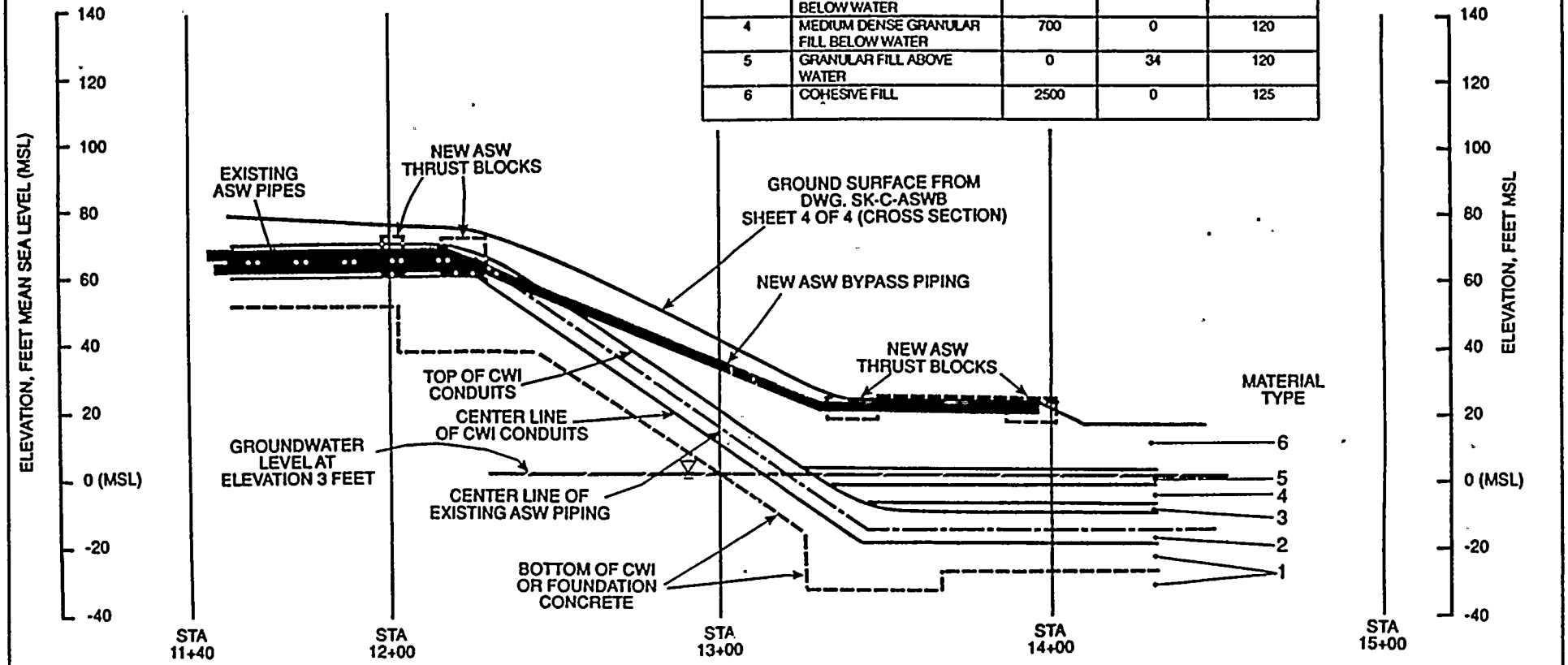

Harding Lawson Associates
Engineering and Environmental Services

CROSS SECTION A - A'
Geotechnical Slope Stability Evaluation
ASW System Bypass
Diablo Canyon Power Plant
San Luis Obisbo County, California

PLATE 2

DRAWN	JOB NUMBER	APPROVED	DATE	REVISED DATE
JMV	10183.ASW-CALC	WAM	5/96	

SURFACE NUMBER	DESCRIPTION	CIRCULAR OR NON-CIRCULAR	FACTOR OF SAFETY
1	TOP OF SLOPE ABOVE ELEVATION 55 FEET	CIRCULAR	6.05
2	FAILURE THROUGH TOE OF SLOPE (CRITICAL FAILURE MODE)	CIRCULAR	3.24
3	FAILURE THROUGH LIQUEFIABLE LAYER BELOW TOE OF SLOPE	NON-CIRCULAR	3.66

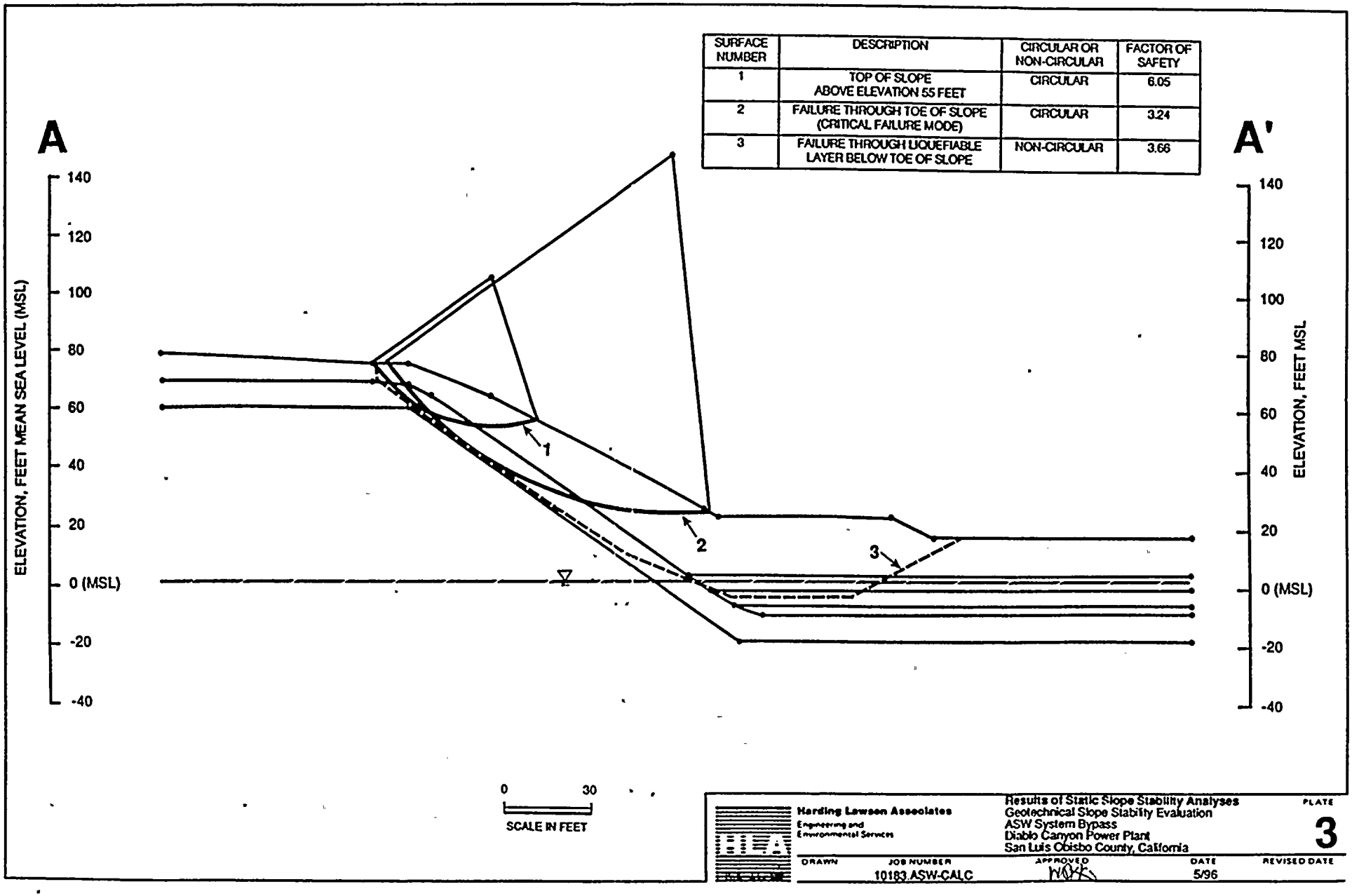

Harding Lawson Associates
Engineering and Environmental Services

Results of Static Slope Stability Analyses
Geotechnical Slope Stability Evaluation
ASW System Bypass
Diablo Canyon Power Plant
San Luis Obisbo County, California

PLATE 3

DRAWN	JOB NUMBER	APPROVED	DATE	REVISED DATE
	10183.ASW-CALC		5/96	

DISTRIBUTION

Geotechnical Slope Stability Evaluation
ASW System Bypass, Unit 1
Diablo Canyon Power Plant
San Luis Obispo County, California

July 3, 1996

5 Copies	Mr. Eric Fujisaki Pacific Gas & Electric Company 245 Market Street, Room 823B N9B San Francisco, California 94106
1 Copy	Mr. Robert Pyke Consulting Engineer 1076 Carol Lane, Suite 136 Lafayette, California 94549

Quality Control Reviewer

Henry T. Taylor
Geotechnical Engineer

Attachment 4.2

Seed, Raymond B. and Leslie F. Harder, Jr., "SPT-based Analysis of Cyclic Pore Pressure Generation and Undrained Residual Strength," from Volume 2, H. Bolton Seed Memorial Symposium, Proceedings, May 1990, Editor J. Michael Duncan, BiTech Publishers Ltd., Vancouver, B.C., Canada

[13] Duncan, J.M., Byrne, P. and Wong, K.S., "Strength, Stress-Strain and Bulk Modulus Parameters for Finite Element Analyses of Stresses and Movements in Soil Masses", Geotechnical Engineering Report No. UCB/CT/80-01, University of California, Berkeley, August 1980.

[14] De Alba, P., Seed, H.B., and Chan, C.K., "Sand Liquefaction in Large-Scale Simple Shear Tests", Journ. Geot. Engrg., ASCE, Vol. 102, No.GT9, Sept. 1976, pp. 909-927.

[15] Seed, H.B. and Lee, K.L., "Undrained Characteristics of Cohesionless Soils", Journ. Soil Mech. and Found. Div., ASCE, Vol. 93, No. SM6, Nov. 1967, pp. 117-141.

[16] OYO Corporation, "First Report on In Situ Site Investigation for Determination of Liquefaction Potential", Prepared for the U.S. National Bureau of Standards, the U.S. Bureau of Reclamation, and the Japanese Public Works Research Institute, March 1984.

17

SPT-Based Analysis of Cyclic Pore Pressure Generation and Undrained Residual Strength

Raymond B. Seed[*] *and Leslie F. Harder, Jr.*[**]

INTRODUCTION

Prominent among Professor Harry Seed's major contributions to geotechnical engineering was the development of methods for evaluation of the seismic stability and performance of dams comprised of, or founded on, soils potentially vulnerable to liquefaction. This subject continued to interest him over the past twenty years, and the analytical procedures which he and his colleagues developed continued to evolve throughout this period. This paper, based on recent studies and work in progress at the time of his death, presents a summary overview of the most current techniques advocated by Dr. Seed and his colleagues for such studies. These will be presented and illustrated by means of application to the re-evaluation of the performance of the Lower San Fernando Dam during the 1971 San Fernando Earthquake, providing a clear demonstration of the methods advocated and facilitating assessment of their performance when applied to this important case history.

SUGGESTED APPROACH

Numerous engineers and investigators have contributed significantly over the past 20 years to the development of the engineering methods described herein. Many of these individuals worked closely with Dr. Seed, while many others worked independently. Though too numerous to individually cite herein, their contributions are gratefully acknowledged.

*Assoc. Prof. of Civil Engineering, University of California, Berkeley, CA 94720. **Supervising Engineer, Calif. Dept. of Water Resources, 1416 Ninth St., Sacramento, CA 94236.

The following procedures for evaluation of the seismic stability and performance of dams comprised of, or founded on, potentially liquefiable soils are evolved from procedures originally developed by Dr. Seed and his colleagues in the early 1970's [1, 2]. The most significant changes since their early inception are: (a) increased reliance on in-situ tests as a primary basis for evaluation of soil conditions, and (b) more recent incorporation of residual or "steady state" strength evaluation as a part of overall stability and performance assessment. Numerous other, more subtle refinements in analytical procedures and recommended correlations will be presented within the context of the overall presentation.

In simple, concise terms, the recommended approach for evaluation of liquefaction potential and seismic stability and performance of dams involves ten basic steps as follow:

1. Determine the cross-section of the dam to be used for analysis.
2. Determine, with the cooperation of geologists and seismologists, the maximum or most severe time history of base excitation to which the dam and its foundation might be subjected.
3. Determine, as accurately as possible, the stresses in the embankment before the earthquake; this is most effectively done using finite element analysis techniques.
4. Determine the dynamic properties of the soils comprising the dam and foundation, such as shear modulus, damping characteristics, and bulk modulus or Poisson's ratio, which determine dynamic response characteristics. Since these material characteristics are nonlinear, it is also necessary to determine how the properties vary with strain.
5. Compute, using an appropriate dynamic finite element analysis procedure, the accelerations and/or dynamic shear stresses induced within the embankment and foundation. For narrow canyons where the ratio of crest length:maximum dam height is less than about 3:1, three-dimensional effects associated with the canyon sidewalls must be accounted for in these analyses. Two-dimensional plane strain dynamic response analyses are sufficient for most dam geometries where crest length is long relative to embankment height. One-dimensional (columnar) analyses are not generally recommended for dynamic response analysis of dams, but can provide sufficiently accurate results for some cases.
6. Evaluate the resistance of potentially liquefiable soil types within the dam and foundation to pore pressure generation under cyclic loading conditions. This is probably most effectively done at this time using Standard Penetration Test (SPT) data, though recent improvements in correlations between SPT and Cone Penetration Tests (CPT) may render CPT a viable alternative when soil conditions and geometry are already well-characterized by means of borings or other information.
7. Based on the results of Steps 6 and 7, evaluate likely pore pressure generation or cyclic strain accumulation within the dam and foundation. This constitutes an evaluation of the potential for "triggering" or initiating soil liquefaction.

8. If pore pressure generation in Step 7 is found to be potentially significant, evaluate the residual undrained ("steady state") strengths of the dam and foundation soils. This is probably most reliably done at present based on SPT data, or on CPT data correlated with SPT-based relationships. Using the resulting residual strengths, evaluate the overall stability of the dam and foundation. This constitutes a "post-triggering" stability evaluation.
9. If Step 6 and/or Step 8 show the dam to be safe with respect to either "triggering" or post-triggering manifestation of major slide movements or deformations, evaluate the magnitude of (limited) overall deformations likely to result from combined static and dynamic loads, and assess their potential impact on dam stability and performance.
10. Be sure to incorporate the requisite amount of judgement in each of the steps (1) through (9), being guided by a thorough knowledge of typical soil characteristics, the essentials of finite element and dynamic response analysis procedures, and a detailed knowledge of the past performance of embankments in other earthquakes.

The importance of engineering judgment at each step cannot be overemphasized. A good example is Step 5: seismic response analyses. At this stage there is always a need to weigh and balance the merits of simplification and associated ease of parameter determination and analysis against the potential loss of accuracy associated with oversimplification. For example, tall dams in narrow canyons are subject to significant 3-D effects associated with the canyon sidewalls, and conventional 2-D plane strain dynamic response analyses can be misleading. On the other hand, fully 3-D response analyses are rendered extremely difficult by the overall size and complexity of the problem, and the inability to generate and develop fully 3-D solutions with a sufficiently "fine" mesh can also adversely impact the results. An optimum solution for some cases can be the use of 2-D, plane strain analyses but with fictitiously high dynamic shear moduli used to model the additional restraint provided by the canyon sidewalls. The resulting calculated dynamic shear strains within the embankment and foundation can then be "post-processed", using the actual (not fictitiously high) dynamic shear moduli, to generate good estimates of the actual, 3-D cyclic shear stresses. This, of course, requires considerable judgment, and it is difficult to reduce such a procedure to a simple set of "rules".

Similarly, at the other extreme, simple one-dimensional (columnar) dynamic response analyses can provide sufficiently accurate cyclic shear stresses as to represent a reliable basis for liquefaction analyses for some cases. Though these simplistic analyses tend to provide notoriously poor predictions of accelerations, strains and cyclic stresses near the crest and sloping faces of dams (due to their inability to correctly model the local problem geometry and/or "topographic amplification"), they can provide reasonably accurate estimates of cyclic shear stresses deep within the interior of an embankment or its foundation, especially one with relatively flat face slopes and a high ratio of crest length to dam height.

THE LOWER SAN FERNANDO DAM SLIDE OF FEBRUARY 9, 1971

The Lower San Fernando Dam in California developed a major slide in the upstream slope and crest as a result of the 1971 San Fernando earthquake ($M_L \approx 6.6$). An investigation of the slide, including trenches and borings, in situ density tests, undisturbed sampling, index testing, static and cyclic load testing, and analyses was performed and reported by Seed et al. [1, 3, 4] and Lee et al. [5]. The field investigation showed that the slide occurred due to liquefaction of a zone of sandy and silty hydraulic fill near the base of the upstream shell.

Two cross sections of the Lower San Fernando Dam are presented in Fig. 1, one showing the observations made in a trench excavated through the slide area and the other showing a reconstructed cross section of the dam, illustrating the zone in which liquefaction occurred. Large blocks of essentially intact soil from the upstream section of the dam moved into the reservoir, riding over or "floating" on the liquefied soil. After movements stopped, the liquefied soil was found to have extruded out below the toe of the dam and up between the intact blocks, with maximum movements as much as 200 ft (61 m) beyond the toe of the dam. The block of soil which contained the toe of the dam moved about 150 ft (46 m) into the reservoir.

Data from seismoscopes located on the abutment and on the crest of the embankment indicated peak accelerations of about 0.55g at both locations, and an analysis of the seismoscope record on the dam crest indicated that the slide occurred about 20 to 30 seconds after the earthquake shaking had stopped. Thus the large slide movements apparently developed in the absence of earthquake-induced stresses and were caused only by the static stresses due to the weight of the materials in the embankment. It can thus be inferred that the earthquake shaking triggered a loss of strength in the soils comprising the embankment and that it was this loss of strength, rather than the inertia forces induced by the earthquake shaking, which led to the sliding of the upstream slope.

While it is readily apparent that sliding due to liquefaction occurred in the upstream shell of the embankment, performance data from the files of the City of Los Angeles Department of Water and Power show that the water levels measured in wells installed in the downstream shell showed only small changes in elevation as a result of the earthquake shaking [6]. These wells readings were obtained one full day after the earthquake, and so did not provide a reliable indication of peak pore pressure development. Nonetheless, the well readings, along with the absence of significant deformations of the downstream shell of the dam, appear to indicate that while the earthquake may have caused at least some increase in pore pressure ratio in the downstream shell and its foundation, there was no significant extent of soil liquefaction in the downstream portion of the hydraulic fill.

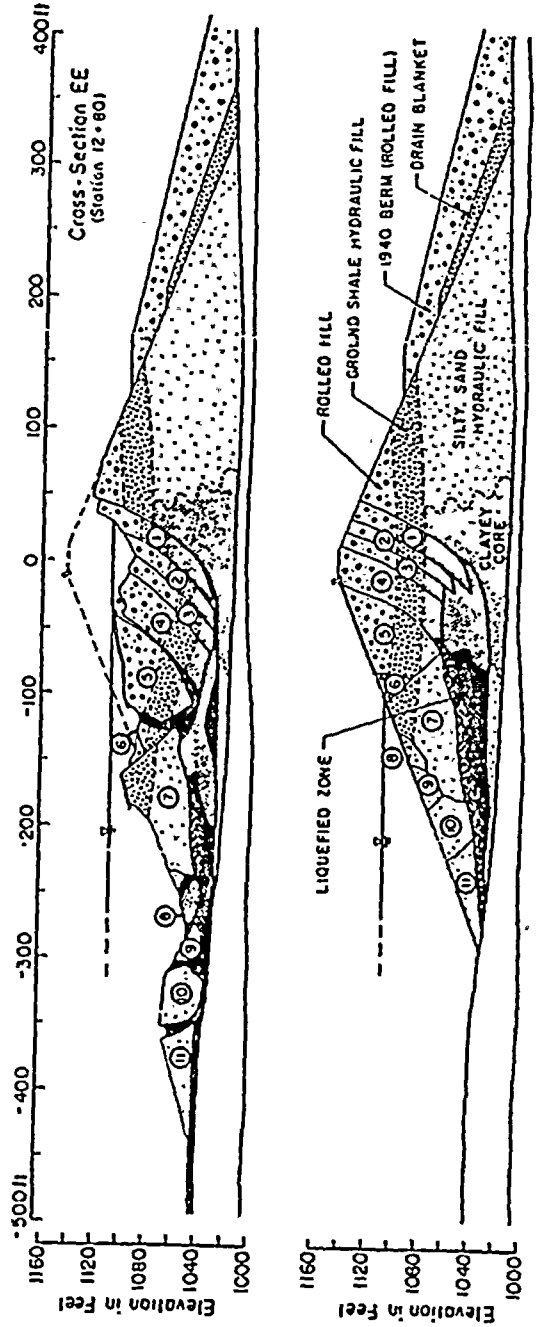

Fig. 1: Cross-Section Through the Lower San Fernando Dam Showing: (a) Conditions After the 1971 Earthquake, and (b) A Schematic Reconstruction of the Failed Cross-Section

This slide represents a uniquely important case history for calibration and verification of liquefaction and seismic stability analysis methodologies for slopes and embankments. Historical construction records as well as extensive post-earthquake geotechnical investigations provide unusually good information regarding embankment and foundation geometry and soil conditions. Instrumental recordings provide a good basis for development of input accelerations, as well as for evaluation of the results of dynamic response analyses. Most important of all, however, is the fact that the largely similar upstream and downstream zones of the dam behaved in highly dissimilar fashion, with the upstream section sliding more than 100 feet into the reservoir, while the downstream section remained stable and experienced only minor deformations of less than a foot at most locations. Accordingly, using well-defined conditions, a reliable analysis methodology must be able to use the relatively minor differences between the upstream and downstream portions of the dam as a basis for accurately predicting these significantly different observed modes of performance.

THE LOWER SAN FERNANDO DAM

The internal geometry and soil conditions within the dam and foundation are well-established as a result of extensive geotechnical studies performed in the early 1970's, and a second set of studies performed over the past five years [1, 5, 6, 7, 8]. Figure 1(b) shows a typical cross-section through the Lower San Fernando Dam as it existed immediately prior to the 1971 earthquake. Embankment construction began in 1912. The embankment was founded on an alluvial foundation consisting primarily of stiff clayey soils with layers and lenses of sand and gravel.

The majority of the embankment consists of hydraulic fill placed between 1912 and 1915. This material was sluiced from the floor of the reservoir and discharged from starter dikes on the upstream and downstream edges of the embankment. The actual dimensions of these starter dikes are unknown. The hydraulic fill process resulted in upstream and downstream shells consisting primarily of sands and silts and a central core consisting primarily of clayey soils. Construction photos of the hydraulic fill placement and past reports indicate that the upstream and downstream sections were raised symmetrically and constructed in a similar manner. Therefore, it is reasonable to assume that the general characteristics of the upstream and downstream hydraulic fill shells are similar.

A 10- to 15-foot-thick hydraulic fill layer consisting of "ground-up" shale from the left abutment was placed in 1916 over the initial hydraulic fill described above. Limited sampling of the ground shale in 1985 disclosed a widely graded sand and silty sand, and construction records indicate that the maximum particle size of the ground shale was about 3 inches.

The embankment was raised a number of times between 1916 and 1930 by placement of rolled fills. The maximum height of the embankment of about 140 feet was reached in 1930. A thin blanket was placed on the lower part

of the downstream slope in 1929 and 1930, apparently for seepage control and to provide additional stability due to the raising of the crest. The composition of the blanket was described in a post-construction report as a mixture of shale and gravelly material placed in 12-inch layers and compacted by trucks. The final addition to the dam was a 4.5H:1V (rolled fill) berm placed on the downstream slope in 1940.

EVALUATION OF STATIC AND CYCLIC STRESSES

An early stage of the analysis process involves evaluation of the static stress conditions within the embankment and foundation. These are important in two ways within the overall analytical scheme: (a) static stresses, especially effective confining stresses, can significantly influence dynamic response characteristics (e.g. dynamic shear moduli), and so can influence cyclic stress calculations, and (b) static stresses, principly the effective (vertical) overburden stress (σ'_o) and the static "driving" shear stress on a horizontal plane (τ_{hv}) can exert a significant influence on the resistance to pore pressure generation or "triggering" of liquefaction at any point within the embankment.

Seed et al. [1] presented results of static finite element analyses of Lower San Fernando Dam performed using the computer program ISBILD [9]. A second, more recent analysis performed in 1987 is presented by Seed et al. [6, 10], using the finite element mesh shown in Figure 2. Both analyses used similar modelling procedures, and both yielded similar results. This type of analysis is, in general, relatively insensitive to choice of computer code, solution methodology, and even type of constitutive model. There are, however, several vital components to such an analysis: (1) nonlinear, stress and stress-level dependent soil behavior must be adequately modelled, (2) soil model parameters must provide adequate modelling of the in situ soils, and (3) hydraulic forces (e.g. bouyancy and seepage gradients) must be included in the analyses.

The 1987 analyses used the program FEADAM84 [11], a 2-D plane strain finite element code. Nonlinear soil behavior was modelled with the "hyperbolic" model proposed by Duncan et al. [12], as modified by Seed and Duncan [11, 13]. The analysis modelled construction of the embankment in a series of "steps", placing new elements in the actual construction sequence.

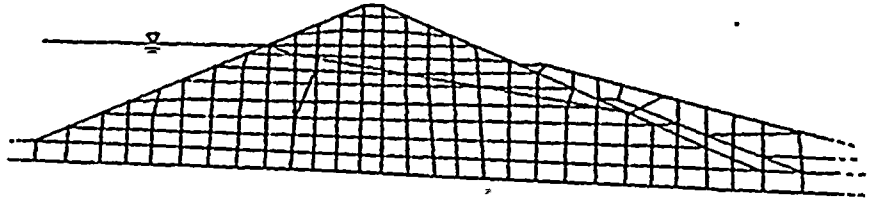

Fig. 2: Finite Element Mesh - Lower San Fernando Dam

Soils below the water table were modelled using effective or "bouyant" unit weights to account for bouyancy in evaluating effective stresses. The effects of seepage forces were evaluated based on an initial flownet analysis from which seepage forces were derived; these were then applied as equivalent nodal forces. The final calculated effective stresses within each element provided the key static stresses (σ'_o and τ_{hv}) necessary for subsequent stages of the overall analytical process.

Seed et al. [1, 4] presented dynamic response analyses of the Lower San Fernando Dam performed in 1972 using the program QUAD4 [14]. Similar analyses were performed more recently using the code FLUSH [15], and the mesh illustrated in Figure 2. Both analyses used static stresses, calculated as described above, as a basis for modelling dynamic shear moduli of cohesionless zones, though slightly different relationships were used to model the nonlinear relationships between shear strain and dynamic shear modulus and damping: [16] for the earlier analyses, and [17] for the more recent analyses. Similarly, the relationships proposed in [16] were used to model strain-dependent moduli and damping in the cohesive zones in the earlier analyses, and [18] in the more recent analyses.

The earlier analyses used the input motions described by Seed et al. [1, 4]: (a) an interpretation of the abutment record by Scott [19], and (b) a modified version of the time history recorded at the Pacoima station during the 1971 San Fernando earthquake. The modifications consisted of trimming of acceleration pulses of greater than 0.9 g, then scaling the record to a maximum horizontal acceleration of 0.6 g, providing a motion in good agreement with Scott's [20] interpretation of the 1971 seismoscope record from the abutment of the Lower San Fernando Dam, but without the unusual low frequency components of the interpreted abutment record. The more recent analyses employed the modified Pacoima input motion scaled to 0.55 g.

The results of the 1973 and 1987 analyses were in close agreement: both produced maximum horizontal crest accelerations on the order of 0.5 to 0.55 g, in good agreement with the actual recorded peak crest accelerations. Both analyses also calculated similar peak cyclic horizontal shear stresses ($\tau_{hv,cyclic}$) within the hydraulic fill zones of the embankment.

It is interesting to note that Jong [20] performed one-dimensional, columnar analyses of individual vertical soil columns through the embankment using the program SHAKE [21]. These analyses, modelling vertical propagation of shear waves and using the same nonlinear soil models and soil parameters as the 2-D FLUSH analyses, significantly underestimated both accelerations and cyclic shear stresses near the crest and upper faces of the embankment. These analyses also, however, provided relatively good agreement with the 2-D dynamic response analyses with regard to cyclic shear stresses ($\tau_{hv,cyclic}$) within the hydraulic fill zones near the base of the embankment, typically calculating peak cyclic shear stresses only 5% to 15% lower than those calculated by the 2-D analyses in these zones.

EVALUATION OF LIQUEFACTION RESISTANCE

Having calculated the cyclic shear stresses resulting from the earthquake loading at each point within the hydraulic fill, the next step is to evaluate the resistance of this material to cyclic pore pressure generation or accumulation of cyclic shear strain. This constitutes evaluation of the resistance to "triggering" or initiation of potential liquefaction failure, defined as sufficient pore pressure or strain accumulation to bring the material to a condition at which undrained residual (or "steady state") strength will control further behavior.

Figure 3 shows a recommended relationship between "corrected" SPT penetration resistance and the equivalent uniform cyclic stress ratio required to "trigger" liquefaction during an earthquake with a duration (or number of loading cycles) representative of a typical earthquake with a magnitude of $M \approx 7\frac{1}{2}$, as suggested by Seed et al. [22, 23]. In this relationship, cyclic stress ratio (CSR) is defined as the ratio of the cyclic shear stress acting on a horizontal plane ($\tau_{hv,c}$) to the initial (pre-earthquake) effective vertical or overburden stress (σ'_o), as CSR = $(\tau_{hv,c})/\sigma'_o$. The relationships presented in Figure 3 represent a significant improvement over earlier, similar relationships developed by Dr. Seed and his colleagues, as (a) they directly account for the influence of fines content on the relationship between penetration resistance and liquefaction resistance, and (b) they are based on a "corrected" or "standardized" SPT penetration resistance.

The standardized penetration resistance $(N_1)_{60}$ is a new "standard" SPT blowcount, based on standardized equipment and procedures as presented (in part) in Table 1 [22, 23]. The use of other types of hammer (e.g. donut hammers), or other types of mechanisms to raise and drop the hammer (e.g. automatic mechanical "trip" hammers, "free fall" hammers, rope and cathead with three turns of the rope about the cathead, etc.), can impart different levels of energy to the top of the drill stem. These non-standard procedures and equipment require correction of the blowcounts in order to develop the standardized blowcount. The $(N_1)_{60}$ "standardized" system and procedures, combined with a "typical" rope and cathead system (with two turns of the rope about the cathead) typically deliver approximately 60% of the theoretical "free fall" hammer energy to the drill stem. For other systems, the measured penetration resistances (N, blows/ft) should be corrected as

$$N_{60} = N \times \frac{ER}{60\%}$$

where ER or energy ratio is the "efficiency" or percent of theoretical free fall energy delivered by the hammer system actually used to the top of the drill stem. This can be measured directly, using a pile analyzer, or can be estimated (for the most common alternate systems in widespread use) based on correlations and data summarized by Seed et al. [22, 23].

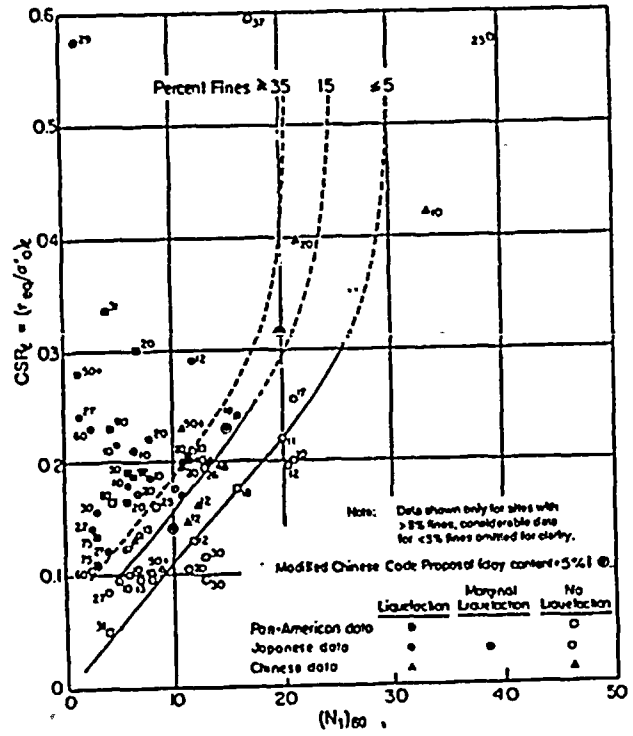

Fig. 3: Relationship Between Cyclic Stress Ratio Causing Liquefaction and N_1-Values for M = 7½ Earthquakes (After Seed, et al., 1984)

Table 1: Recommended "Standardized" SPT Equipment and Procedures (After Seed, et al., 1984)

Sampler:	Std. Sampler with: (a) O.D. = 2.00 inches, and (b) I.D. = 1.375 inches (constant - i.e. no room for liners in the barrel.)
Drill Rods:	A or AW for depths less than 50 feet N or NW for greater depths
Energy Delivered to Sampler:	2520 in.-lbs. (60% of theoretical free fall maximum.)
Blowcount Rate:	30 to 40 blows per minute
Penetration Resistance Count:	Measured over range of 6 to 18 inches of penetration into the ground

An additional correction, increasing the measured N-value by between 10% to 30%, can be necessitated by the use of an ASTM standard sampler configured to accommodate an internal sample liner (tube), but with the liner ommitted. This is fairly common practice in the U.S., and causes a reduction in frictional drag inside the sampler, lowering the blowcounts by about 10% to 30% (increasing percent change with increased blowcount), as summarized by Seed et al. [22, 23] relative to the blowcounts obtained using a standard sampler with a constant inside diameter of 1.375 inches.

Having made any appropriate corrections necessary to develop the standardized blowcount $(N)_{60}$, this penetration resistance must be further corrected to account for effective overburden stress to develop the final, standardized and corrected penetration resistance $(N_1)_{60}$ representative of the "equivalent" penetration resistance at a hypothetical overburden stress of σ'_o = 1 ton/ft^2 (1 kg/cm^2)as:

$$(N_1)_{60} = N_{60} \times c_N$$

Dr. Seed and his colleagues have long recommended a pair of relationships between σ'_o and c_N; one for sandy soils at $D_R \approx 40$ to 60% and one for $D_R \approx 60$ to 80%, as shown in Figure 4. An alternate relationship, proposed by Liao and Whitman [24] is $c_N = 1/\sqrt{\sigma'_o}$ where σ'_o is expressed in units of [tons/ft^2]. This provides a relationship intermediate between the two suggested relationships shown in Figure 4, and so eliminates the need to estimate D_R. If D_R must be estimated, for in situ, clean sandy soils not placed recently, the approximate relationship presented in Figure 5 can be used as a guide [25]. This relationship should not be used for freshly-placed soils, or for coarser materials than fine to medium sands.

The relationships between $(N_1)_{60}$ and the equivalent uniform cyclic stress ratio necessary to cause liquefaction (CSR_ℓ) in Figure 3 can be extended to earthquakes of magnitude other than M ≈ 7½ by noting that earthquakes of larger magnitude tend to produce a longer duration of shaking and thus more cycles of loading. Seed et al. [26, 27] present procedures for converting a typical, irregular earthquake-induced cyclic load history to an "equivalent" number of uniform loading cycles with an amplitude equal to 65% of the peak or maximum amplitude of the irregular load history. Processing a large number of recorded earthquake time histories using these techniques, Seed et al. [26, 27] developed the "typical" or average numbers of equivalent uniform loading cycles for different magnitude events shown in Table 2.

For earthquakes of magnitude not equal to 7½, the value of CSR_ℓ determined from Figure 3 can be corrected to develop an estimate of the CSR necessary to cause liquefaction as

$$CSR_{\ell(M=M)} = CSR_{\ell(M=7½)} \cdot C_M$$

where C_M values are a function of magnitude, as suggested by the first and third columns of Table 2. These values are based on review of a considerable body of laboratory test data [26]. An alternate procedure would be to develop an estimate of the number of equivalent, uniform

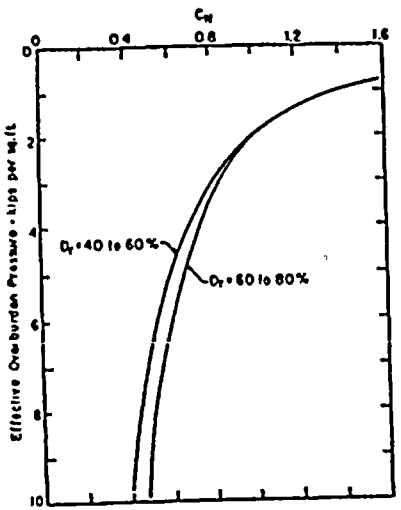

Fig. 4: Chart for Values of C_N

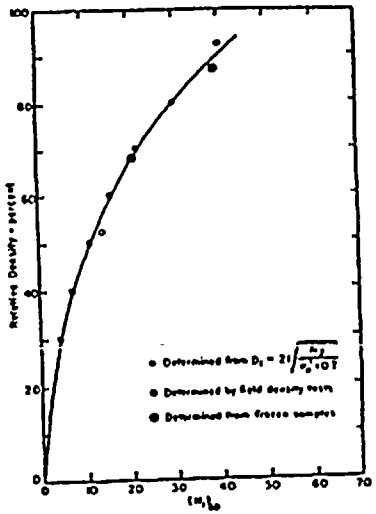

Fig. 5: Approximate Relationship Between D_R and $(N_1)_{60}$ [25]

Table 2: Relationship Between Magnitude, Number of Equivalent Uniform Load Cycles, and Liquefaction Resistance Factor C_M

Earthquake Magnitude, M	No. of representative cycles at 0.65 $\tau_{cyclic, max}$	Magnitude or Duration Correction Factor: C_M
8 1/2	26	0.89
7 1/2	15	1.0
6 3/4	10	1.13
6	5-6	1.32
5 1/4	2-3	1.5

loading cycles representing the earthquake in question (after Seed et al., [27]), and then use the second and third columns of Table 2 to select an appropriate value of C_M. Either of these procedures result in relationships between $(N_1)_{60}$ and CSR_ℓ for earthquakes of other magnitudes than $M \approx 7\frac{1}{2}$ that are in good agreement with available field data [22, 23], though the field (case history) data base is less extensive for events of other ranges of magnitude.

Virtually all of the field (case history) data reflected in Figure 3 (and in similar collections of data for other magnitude ranges) are for level ground conditions and relatively shallow soils with relatively small initial effective

overburden stresses. At higher effective overburden stresses, a given CSR and number of loading cycles will be more damaging. This is because while soils generally develop higher cyclic load resistance with increasing confinement, the normalized resistance as expressed in terms of cyclic stress ratio usually decreases with increasing confinement. Accordingly, values of CSR_ℓ from Figure 3 can be used for in situ conditions where $\sigma'_o \leq 1$ ton/ft^2 (1 kg/cm^2), but must be corrected for conditions with initial effective overburden stresses greater than 1 ton/ft^2 as

$$CSR_{\ell(\sigma'_o = \sigma'_o)} = CSR_{\ell(\sigma'_o = 1\,tsf)} \cdot K_\sigma$$

A recommended relationship between K_σ and σ'_o is presented in Figure 6, based on data summarized by Harder [28].

Finally, all of the above has been based on "level ground conditions", or conditions in which there is no static "driving" shear stress acting on a horizontal plane in the soil. Generation of pore pressures and accumulation of shear strains under cyclic loading can be significantly affected by the presence of a static (non-cyclic) driving shear stress, and this too must be accounted for in analysis of liquefaction resistance within dams and embankments.

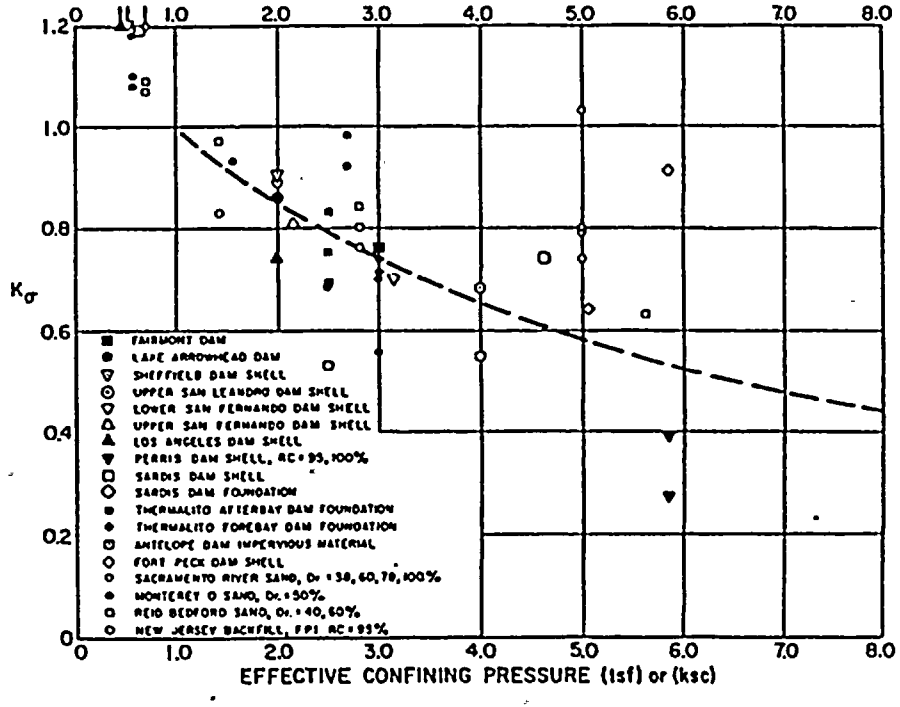

Fig. 6: Relationship Between Effective Vertical Stress (σ'_o) and K_α

Early relationships suggested by Dr. Seed to account for this suggested that the presence of a static driving shear stress on a horizontal plane was strongly beneficial, and that it significantly increased the soil's resistance to liquefaction. This remains true for relatively dense soils, or soils which would tend to dilate under uni-directional shearing. More recent studies, however, have shown that for very loose soils (soils which are less dilatant or more contractive under uni-directional shearing), the presence of a static driving shear stress can actually decrease the resistance of the soil to the initiation of liquefaction. Good data regarding this remains somewhat limited, and further investigations of this would be of significant value. The original method proposed by Seed [29] to account for the effects of driving static shear stresses employed the following equation

$$CSR_{\ell(\alpha = \alpha)} = CSR_{\ell(\alpha = 0)} \cdot K_\alpha$$

(where α is defined as the ratio of static driving shear stress on a horizontal plane to the initial effective overburden stress as $\alpha = \tau_{hv}/\sigma'_o$) Based on data available at this time (data summarized by Harder [28], as well as research in progress), it is suggested that the relationships between α and K_α proposed by Seed [29] be replaced by the relationships presented in Figure 7. These are based on data for conditions where $\sigma'_o \leq 3$ tons/ft^2 (3 kg/cm^2), and are appropriate only for these conditions. At higher initial effective overburden stresses, soils will be less dilatant or more contractive, and K_α values will decrease.

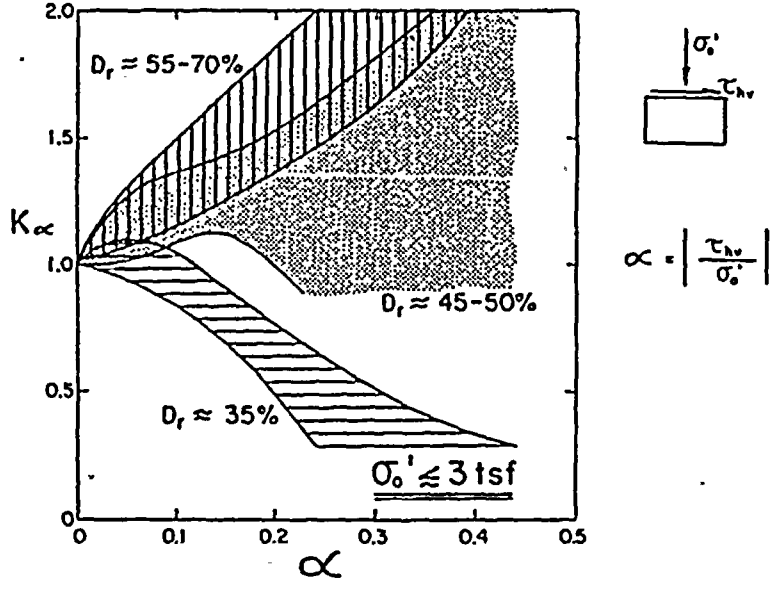

Fig. 7: Relationship Between α and K_α

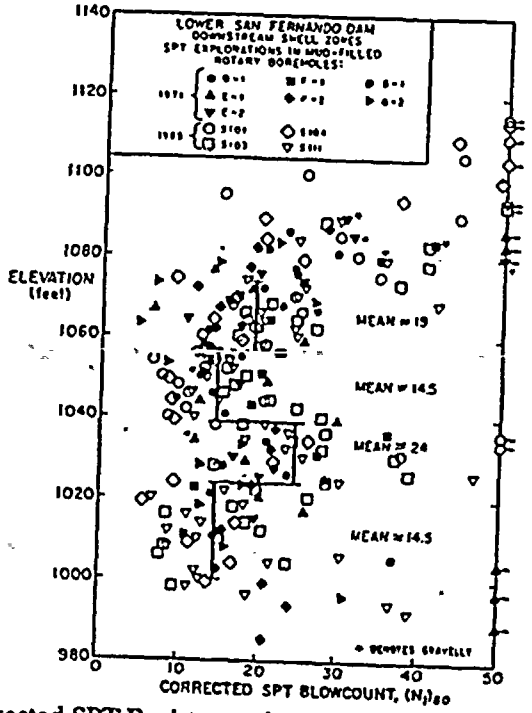

Fig. 8: Corrected SPT Resistances in the Downstream Hydraulic Fill

In summary, the equivalent uniform cyclic stress ratio necessary to cause or "trigger" liquefaction can be determined, based on knowledge of five factors: $(N_1)_{60}$, fines content, the in situ static shear stress (τ_{hv}), the initial effective overburden stress (σ'_o), and the earthquake magnitude or number of equivalent loading cycles.

"TRIGGERING" ANALYSIS

Figure 8 shows the results of Standard Penetration Tests (SPT) performed in cohesionless soils (primarily sands and silty sands) within the hydraulic fill of the downstream section of the Lower San Fernando during the 1971 and 1985 field investigations, all in terms of the corrected blowcounts $(N_1)_{60}$ vs. elevation. No similar tests could be performed in the upstream zone due to the slide damage. The 1971 SPT were performed using a standard safety hammer and rope and pulley, and so required no hammer energy correction. The use of an ASTM sampling tube with liners omitted, however, required that the resulting N-values be increased by 10% to 30% [22, 23] to develop corrected $(N_1)_{60}$-values. The 1985 SPT data also required a sampler correction, together with a hammer energy correction of 72/60 to account for a measured SPT hammer energy of 72%.

As shown in Figure 8, the resulting $(N_1)_{60}$ values from 1971 and 1985 show similar trends, and the hydraulic fill can be subdivided into four elevation zones of apparently similar properties. Table 3 summarizes the corresponding $(N_1)_{60}$ values within each of these zones. As shown in this table, two elevation zones appear to have significantly lower penetration resistances than the other zones. It should be noted that, although "best estimates" or mean values of $(N_1)_{60}$ are appropriate for these analyses of a case study involving comparison with observed field performance, more conservative (lower than mean) values would normally be selected for analyses performed in order to predict the likely future behavior of any given dam or embankment.

The $(N_1)_{60}$ values summarized in the second column of Table 3 are based on post-earthquake blowcounts, and some correction is required to account for densification likely to have occurred due to the earthquake shaking. Seed et al. [6] have estimated that the pre-earthquake blowcounts in the downstream hydraulic fill would have been lower, on the average, by about 2 blows/ft, and this is reflected in the third column of Table 3 which will be taken as the values for the downstream zones in these analyses.

There is some minor question as to how these values should be extrapolated to the upstream portion of the hydraulic fill within which the slide occurred. Similarity and uniformity of construction procedures support the use of the same $(N_1)_{60}$ values for the upstream section. On the other hand, it has been suggested that the upstream section may have been somewhat less densely consolidated due to reservoir bouyancy and the absence of the downstream berms. If reservoir filling had been initiated sufficiently quickly after completion of construction that full consolidation of the embankment under its own weight was not completed, then the maximum difference in density between the upstream and downstream hydraulic fill sections would have been such that the upstream $(N_1)_{60}$ values would need to be reduced by about 1 blow/ft. As shown in Table 3, a reduction of 1 blow/ft will be used for the analyses described herein. It should be noted that this relatively minor decrease in the upstream section's $(N_1)_{60}$ values does not explain the significant differences in performance

Table 3: Representative $(N_1)_{60}$-Values (Blows/ft) Within the Hydraulic Fill Shells of the Lower San Fernando Dam

Elevation (ft)	Representative Post-Earthquake $(N_1)_{60}$-Values: Downstream Section	Representative Pre-Earthquake $(N_1)_{60}$-Values: Downstream Section	Representative Pre-Earthquake $(N_1)_{60}$-Values: Upstream Section
1074-1057	19	17	16
1056-1039	14.5	12.5	11.5
1038-1024	24	22	21
1023-1000	14.5	12.5	11.5

between the upstream and downstream sections. Instead, these differences in performance are much more strongly influenced by: (a) the lighter effective overburden stresses in the upstream section, which cause the earthquake-induced cyclic stress ratios to be larger here than in the downstream section, and (b) the higher α values in the downstream section, due primarily to the effects of seepage forces within the embankment.

In addition to establishing representative $(N_1)_{60}$-values for the hydraulic fill zones, it is also necessary to select representative fines contents for the materials in these zones (percent by dry weight finer than a #200 sieve). This is complicated by the tremendous variability of the gradations of these materials, and their variability over small distances, both of which are a natural consequence of the hydraulic fill process. Materials present range from clean sands and gravelly sands, through silty sands and sandy silts, to pure silts and even clayey silts. Vertical striations, or abrupt changes in gradation, occur over intervals of only a few centimeters or less. Nonetheless, considering the overall nature of the hydraulic fill in the zones of interest, a representative fines content of about 25% to 35% was selected for these analyses.

The upstream and downstream hydraulic fill zones (excluding the more cohesive core which was judged not to be susceptible to liquefaction due to the primarily clayey soils present) was divided into four elevation zones, as shown in Figure 9 and Table 3. These zones were then subdivided into "elements", as illustrated in Figure 9, and an evaluation of the likelihood of initiating or "triggering" liquefaction within each element was performed, using the information generated from all previous steps of the analyses described up to this point.

As an example, consider the element in the upper level of the upstream hydraulic fill zone immediately adjacent to the "clayey core" in Figure 9. The static driving shear stress and effective overburden stresses were calculated (in the 1987 static stress analyses described previously) to be τ_{hv} = 780 lb/ft^2 and σ'_o = 5,280 lb/ft^2, so that α = 780/5,280 = 0.147. As $(N_1)_{60} \approx 16$ blows/ft in this zone, with fines content $\approx$ 25% to 35%, the equivalent uniform cyclic stress ratio necessary to cause liquefaction in shallow, level ground conditions and a magnitude 7½ earthquake (from Figure 3) is CSR $\approx$ 0.275. This must be adjusted for: (a) the magnitude of the San Fernando Earthquake ($M \approx 6.6$) based on Table 2, (b) the effects of driving static shear stress ($\alpha \approx 0.15$) based on Figure 7, and (c) the effects of overburden stress according to Figure 6 as

$$CSR_{\ell,field} = CSR_{\ell} \times C_M \times K_\alpha \times K_\sigma = (0.275)(1.15)(1.2)(0.76) = \underline{0.288}$$

The peak cyclic shear stress on a horizontal plane in this element was found, from the recent dynamic response analyses described previously, to be $\tau_{hv,cyclic,max} \approx$ 1,845 lb/ft^2. Using 65% of this to establish the corresponding equivalent uniform cyclic stress ratio

$$CSR_{eq} \approx \frac{0.65 \times \tau_{hv,c,max}}{\sigma'_o} = \frac{(0.65)(1{,}845\ \text{lb/ft}^2)}{(5{,}280\ \text{lb/ft}^2)} = \underline{0.227}$$

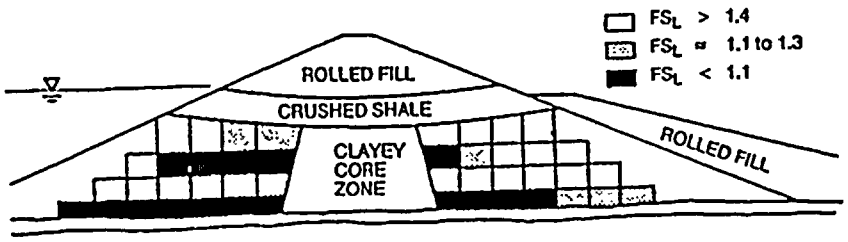

Fig. 9: Results of Analyses of Resistance to Initiation or "Triggering" of Liquefaction Failure - Lower San Fernando Dam

Comparing the equivalent, uniform, earthquake-induced cyclic stress ratio (CSR_{eq}) with the uniform cyclic stress ratio necessary to fully trigger liquefaction, the factor of safety against "triggering" can be calculated as

$$FS_\ell = \frac{CSR_{\ell,field}}{CSR_{eq}} = \frac{0.288}{0.227} = \underline{1.27}$$

This factor of safety can be interpreted in a number of ways. Figure 10 shows a plot of residual excess pore pressure ratio ($r_u = \Delta u/\sigma'_o$) based on laboratory test data for level ground conditions ($\alpha = 0$) as summarized by Tokimatsu and Yoshimi, [30] for sandy soils, and Evans [31] and Hynes [32] for gravelly soils, as summarized by Marcuson and Hynes [33]. For non-level ground conditions ($\alpha \neq 0$), the effective vertical stress need not necessarily be fully eliminated by pore pressure increases to initiate "large" deformations in the presence of combined cyclic and "driving" static shear stresses. Accordingly, when $\alpha \neq 0$, the residual excess pore pressure ratio is best defined as the ratio of cyclically-generated pore pressures (Δu) to the value of Δu necessary to initiate large deformations ($\Delta u_{\ell im}$) as

$$r_{u\alpha\neq 0} = \frac{\Delta u}{\Delta u_{\ell im}}$$

Less data is available regarding the relationships between r_u and FS_ℓ for non-level ground conditions, and differences of opinion exist as to how this data can best be interpreted. Much of this is due to uncertainty regarding the nature of the transition from a condition wherein cyclic pore pressure generation (or cyclic strain accumulation) behavior exerts primary control on performance, to "post-triggering" conditions wherein undrained residual (or "steady state") strengths control behavior.

Nonetheless, at this time it appears that a reliable analysis can be performed by considering that:

1. Soil elements with low factors of safety ($FS_\ell \leq 1.1$) would achieve conditions wherein soil liquefaction failure should be considered to have been "triggered", and undrained residual strengths (S_r) should be assigned to these zones for further stability and deformation analyses.

2. Soil elements with a high factor of safety ($FS \geq 1.4$) would suffer relatively minor cyclic pore pressure generation, and should be assigned some large fraction of their static strength for further stability and deformation analyses.

3. Soil elements with intermediate factors of safety ($FS \approx 1.1$ to 1.4) should be assigned strength values somewhere between (though in some cases including) the values appropriate to conditions 1 and 2 above. Whether the values assigned should be nearer to the initial static strength or to the residual undrained strength is a function of FS_ℓ, whether or not the soil is judged to be strongly contractive in uni-directional shearing (and thus potentially vulnerable to "progressive" failure), and levels of uncertainty involved in various steps of the analysis up to this point (for any specific case).

For these analyses of the Lower San Fernando Dam, elements with: (a) $FS \leq 1.1$ will be assigned residual undrained strengths, (b) $FS \geq 1.4$ will be assigned 75% of their (drained) static strength, and (c) $1.1 \leq FS \leq 1.4$ will be assigned strengths developed by interpolation, as a function of FS_ℓ, between conditions (a) and (b). Figure 9 shows the distribution of FS_ℓ within the critical hydraulic fill zones.

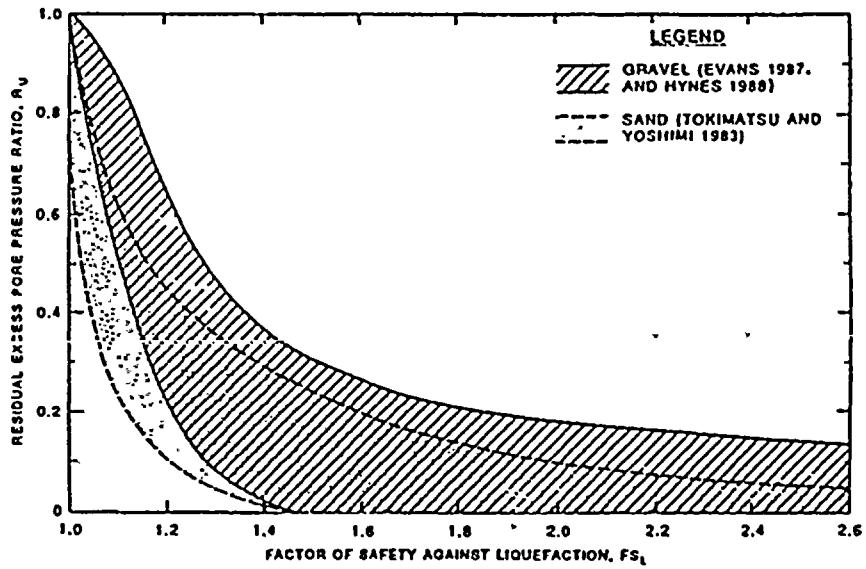

Fig. 10: Typical Relationships Between Residual Excess Pore Pressure Ratio and Factor of Safety Against Liquefaction; From Laboratory Data (Marcuson and Hynes, 1989)

EVALUATION OF UNDRAINED RESIDUAL STRENGTH

As early as 1936, Casagrande [34] postulated that soils sheared under undrained conditions would achieve a residual condition at which further shearing would cause no additional change in strength or volume or pore pressure. This principle is the underlying basis of "critical state" soil mechanics [35] as well as recently proposed "steady state" analysis techniques for evaluation of "post-triggering" stability of liquefiable soils.

Poulos and Castro [36] recently proposed a methodology for evaluation of in situ undrained residual "steady state" strengths (S_{us}), based on obtaining high quality soil samples with minimal disturbance, testing these in the laboratory, and then using specially developed techniques to correct the resulting laboratory S_{us} values for the effects of void ratio changes due to sampling, handling and test set-up in order to develop estimates of the field (in situ) S_{us}. This represents a major contribution to geotechnical practice, as it has spurred considerable interest and research into the use of residual undrained strengths for post-liquefaction stability assessment. Unfortunately, due to the very high sensitivity of S_{us} to even small changes in void ratio, these techniques for laboratory-based evaluation of S_{us} do not presently appear to represent a reliable basis for engineering analyses, unless very conservative assumptions and large factors of safety are employed to account for the considerable uncertainties involved [6, 33].

Dr. Seed recommended an alternate technique for evaluation of in situ undrained residual strength (S_r) based on Standard Penetration testing [37]. He presented the results of back-analyses of a number of liquefaction failures from which values of the residual undrained strength could be calculated for soil zones in which SPT data was available, and proposed a correlation between S_r and $(N_1)_{60\text{-}cs}$. $(N_1)_{60\text{-}cs}$ is a "corrected" penetration resistance, as discussed previously, but with an additional correction for fines content to generate an equivalent "clean sand" blowcount as

$$(N_1)_{60\text{-}cs} = (N_1)_{60} + N_{corr}$$

where N_{corr} is a function of percent fines, as shown in Table 4. It should be noted that this is not the same "fines" correction as is used in the "triggering" analyses (e.g. Figure 3).

Table 4: Recommended Fines Correction for S_r Evaluation Using SPT Data

Percent Fines	N_{corr} (blows/ft)
10%	1
25%	2
50%	4
75%	5

Figure 11 presents an updated correlation between S_r and $(N_1)_{60\text{-}cs}$, based on values back-calculated from an increased number of case studies, as listed in Table 5. Many of the S_r values presented are slightly different from those originally presented [37] as: (a) improved techniques have been used to account for dynamic effects (e.g. momentum) in developing estimates of S_r from the field failures, and (b) additional data has recently become available regarding several of these case studies. It is recommended that the lower-bound, or near lower-bound relationship between S_r and $(N_1)_{60\text{-}cs}$ in Figure 11 be used for residual undrained strength analyses at this time owing to scatter and uncertainty, and the limited number of case studies back-analyzed to date.

Assigning "post-triggering" analysis strengths to the various soil elements of Figure 9, based on FS_r and Figures 10 and 11, the resulting post-earthquake static factor of safety for the most critical failure surface in the upstream portion of the dam is considerably less than 1.0, indicating the onset of major slide movements, in good agreement with the actual observed performance. It is interesting to note that the actual residual undrained strength of the lower zone of the upstream hydraulic fill (with $(N_1)_{60} \approx 11.5$, and $(N_1)_{60\text{-}cs} \approx 13.5$ blows/ft) was judged to have been on the order of $S_r \approx 300$ to 500 psf, as shown in Table 5 and Figure 11. Assigning

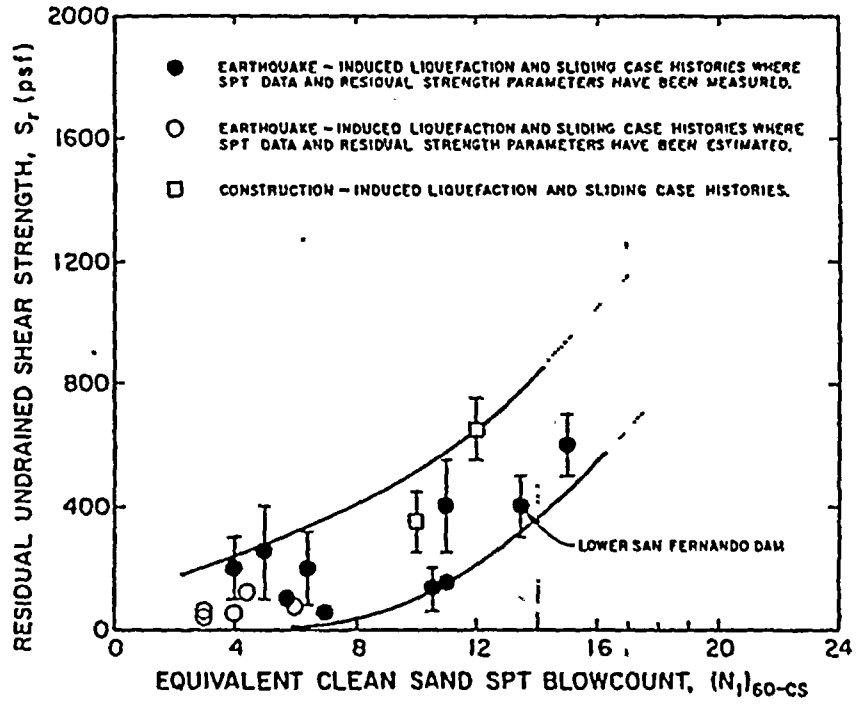

Fig. 11: Relationship Between Corrected "Clean Sand" Blowcount $(N_1)_{60\text{-}cs}$ and Undrained Residual Strength (S_r) from Case Studies

Table 5: Undrained Residual Strength (S_r) vs. Corrected Penetration Resistance $(N_1)_{60\text{-}cs}$ Based on Analyses of Case Histories

Structure or Earth Structure	Apparent Cause of Sliding	Representative $(N_1)_{60}$ (blows/ft)	Fines Content (%)	Representative $(N_1)_{60\text{-}CS}$ (blows/ft)	Estimated Residual Undrained Shear Strength, S_r (lb/ft^2)	References
Calaveras Dam	1918 Construction			12[a]	650±50	37,40
Sheffield Dam	1925 Santa Barbara Eq. (M=6.3)			6[a]	75±25	37
Fort Peck Dam	1938 Construction			10[a]	250±100	37,39,40
Solvarra Canal Dike	1940 El Centro Eq. (M=7.2)			4[a]	50±25	37,44
Lake Merced Bank	1957 San Francisco Eq. (M=5.7)	6	3	6	100	37,46
Kawaguchi-Cho Building	1964 Niigata Eq. (M=7.5)			6[a]	120	37
Ueno Railway Embankment	1964 Niigata Eq. (M=7.5)			3[a]	40	37
Snow River Bridge Fill	1964 Alaskan Eq. (M=8.5)			7	30	37,47
Koda Numa Railway Embankment	1968 Tokachi-Oki Eq. (M=7.9)			3[a]	50	37
San Fernando Juvenile Hall	1971 San Fernando Eq. (M=6.6)	6	65	10.5	150±70	37,38,40
Lower San Fernando Dam	1971 San Fernando Eq. (M=6.6)	11.5	25	13.5	400±100	6
Upper San Fernando Dam	1971 San Fernando Eq. (M=6.6)	13	25	15	600±100	42
Mochi-Koshi Tailings	1978 Izu-Oshima Eq. (M=7.0)	0	80	5	250±150	37,39,40, 43,44,45
Whiskey Springs Fan	1983 Borah Peak Eq. (M=7.3)	8[b]	40[b]	11	150±10	28
La Marquesa Dam - U/S Slope	1985 Chilean Eq. (M=7.8)	4	30	6	200±125	41
La Marquesa Dam - D/S Slope	1985 Chilean Eq. (M=7.8)	9	20	11	400±150	41
La Palma Dam	1985 Chilean Eq. (M=7.8)	3	15	4	200±100	41

Notes: a. SPT blowcount estimated from appraisal of relative density.
b. Equivalent SPT blowcount determined from Becker Penetration test performed in silty gravel. Fines content computed for sieves 10 mm size.

reasonable strength values to the upstream toe and overlying soil zones [1, 6], an average residual undrained strength of $S_r \approx 800$ to 900 psf in the upstream hydraulic fill zone would have been required to provide an overall factor of safety equal to one.

Assigning strength values to the various elements in the downstream hydraulic fill zones, using the same procedures, the resulting static factor of safety is well above one (FS ≈ 1.3 to 1.4). Applying Newmark-type seismic displacement analyses [48], as modified by Seed and Makdisi [49, 50], and using these assigned strength values, results in calculation of likely seismic displacements for the downstream section of the dam of on the order of 4 to 30 inches, again in reasonably good agreement with the observed field performance.

SUMMARY AND CONCLUSIONS

The methods presented herein are successfully able to reproduce the observed behavior of the Lower San Fernando Dam during the 1971 San Fernando Earthquake, predicting large slide movements of the upstream section and limited displacements of the downstream section. These analytical methods, coupled with appropriate engineering judgments, appear to provide a sound basis for evaluation of the seismic stability of

dams and slopes comprised of, or founded on, potentially liquefiable sandy and silty soils. This is a tremendous achievement, and the authors applaud Dr. Seed and the many others who have contributed to the development of these procedures over the last 20 years.

This does not mean that further advances would not be highly desirable. There is a need for additional study of the transition from conditions in which cyclic pore pressure generation or cyclic strain accumulation control behavior to conditions in which residual or large-strain strength and deformation characteristics control behavior. Closely related to this issue is the need to further investigate the influence of static "driving" shear stresses, as currently incorporated in the analyses using α and K_α, especially at relatively high initial effective confining stresses. In addition, there is a need to extend these methods to permit similar, reliable analysis of gravelly soils (e.g. recent research involving the use of Becker Hammer large-scale penetration resistance). Finally, additional investigation of the liquefaction resistance of moderately plastic soils, and the influence of clayey fines on liquefaction resistance would also be useful.

All of this would please Harry Seed, who so enjoyed the challenges presented by his own geotechnical career and who devoted so much of himself to preparing the next generation for challenges such as these.

REFERENCES

[1] Seed, H. B., Lee, K. L., Idriss, I. M. and Makdisi, F. (1973). "Analysis of the Slides in the San Fernando Dams During the Earthquake of Feb. 9, 1971", Rept. No. UCB/EERC-73/2, Univ. of Calif., Berkeley.

[2] Seed, H. B. and Idriss, I. M. (1971). "A Simplified Procedure for Evaluating Soil Liquefaction Potential", JSMFD, ASCE, Vol. 97, No. SM 9, pp. 1249-1274.

[3] Seed, H. B., Lee, K. L., Idriss, I. M. and Makdisi, F. (1975). "The Slides in the San Fernando Dams During the Earthquake of February 9, 1971", J. of Geot. Engin., ASCE, Vol. 101, No. GT7, pp. 651-688.

[4] Seed, H. B., Lee, K. L., Idriss, I. M. and Makdisi, F. (1975). "Dynamic Analyses of the Slide in the Lower San Fernando Dam During the Earthquake of February 9, 1971", J. of Geot. Engin., ASCE, Vol. 101, No. GT9, pp. 889-911.

[5] Lee, K. L., Seed, H. B., Idriss, I. M. and Makdisi, F. (1975). "Properties of Soil in the San Fernando Hydraulic Fill Dams", J. of Geot. Engin., ASCE, Vol. 101, No. GT8, pp. 801-821.

[6] Seed, H. B., Seed, R. B., Harder, L. F. and Jong, H. L. (1989). "Re-Evaluation of the Slide in the Lower San Fernando Dam in the 1971 San Fernando Earthquake", Rept. No. UCB/EERC-88/04, University of California, Berkeley.

[7] Castro, G., Keller, T. O. and Boynton, S. S. (1989). "Re-Evaluation of the Lower San Fernando Dam. Report 1: An Investigation of the February 9, 1971 Slide", Rept. No. GL-89-2, U.S. Army Corps of Engineers, WES.

[8] Earth Technology Corp. (1985). "Cone Penetration Tests, Lower San Fernando Dam", Report prepared for U.S. Army Corps of Engineers.
[9] Ozawa, Y. and Duncan, J. M. (1973). "ISBILD: A Computer Program for Analysis of Static Stresses and Movements in Embankments During Construction", Geot. Research Rept. No. TE-73-4, University of California, Berkeley.
[10] Jong, H.-L. and Seed, R. B. (1988). "A Critical Investigation of Factors Affecting Seismic Pore Pressure Generation and Post-Liquefaction Flow Behavior of Saturated Soils", Geot. Research Rept. No. SU/GT/88-01, Stanford University.
[11] Duncan, J. M., Seed, R. B., Wong, K. S. and Ozawa, Y. (1984). "FEADAM84: A Computer Program for Finite Element Analysis of Dams", Geot. Research Rept. No. SU/GT/84-03, Stanford University.
[12] Duncan, J. M., Byrne, P., Wong, K. S. and Mabry, P. (1980). "Strength, Stress-Strain and Bulk Modulus Parameters for Finite Element Analyses of Stresses and Movements in Soil Masses", Geot. Research Rept. No. UCB/GT/80-01, Univ. of California, Berkeley.
[13] Seed, R. B. and Duncan, J. M. (1983). "Soil-Structure Interaction Effects of Compaction-Induced Stresses and Deflections", Geot. Research Rept. No. UCB/GT/83-06, Univ. of California, Berkeley.
[14] Idriss, I. M., Lysmer, J., Hwang, R. N. and Seed, H. B. (1973). "QUAD4: A Computer Program for Evaluating the Seismic Response of Soil Structures by Variable Damping Finite Element Procedures," Rept. No. UCB/EERC-73/16, Univ. of California, Berkeley.
[15] Lysmer, J., Udaka, T., Tsai, C.-F. and Seed, H. B. (1975). "FLUSH: A Computer Program for Approximate 3-D Analysis of Soil-Structure Interaction Problems", Rept. No. UCB/EERC-75/30, Univ. of California, Berkeley.
[16] Seed, H. B. and Idriss, I. M. (1970). "Soil Moduli and Damping Factors for Dynamic Response Analysis", Rept. No. UCB/EERC-70/10, Univ. of California, Berkeley.
[17] Sun, J. I., Golesorkhi, R. and Seed, H. B. (1988). "Dynamic Moduli and Damping Ratios for Cohesive Soils", Rept. No. UCB/EERC-88/15, Univ. of California, Berkeley.
[18] Seed, H. B., Wong, R. T., Idriss, I. M. and Tokimatsu, K. (1984). "Moduli and Damping Factors for Dynamic Analyses of Cohesionless Soils", Rept. No. UCB/EERC-84/14, Univ. of California, Berkeley.
[19] Scott, R. F. (1972). "The Calculation of Horizontal Accelerations from Seismoscope Records", Paper presented at a Seismological Society of America Conference in Hawaii.
[20] Jong, H.-L. (1988). "A Critical Investigation of Post-Liquefaction Strength and Steady-State Flow Behavior of Saturated Soils", Ph.D. Thesis, Dept. of Civil Engin., Stanford University.
[21] Schnabel, P. B., Lysmer, J. and Seed, H. B. (1972). "SHAKE: A Computer Program for Earthquake Response Analysis of Horizontally Layered Sites", Rept. No. UCB/EERC-72/12, Univ. of California, Berkeley.

[22] Seed, H. B., Tokimatsu, K., Harder, L. F. and Chung, R. (1984). "The Influence of SPT Procedures in Soil Liquefaction Resistance Evaluations", Rept. No. UCB/EERC-84/15, Univ. of California, Berkeley.
[23] Seed, H. B., Tokimatsu, K., Harder, L. F. and Chung, R. (1985). "Influence of SPT Procedures in Soil Liquefaction Resistance Evaluations", JGED, ASCE, Vol. 111, No. 12.
[24] Liao, S. C. and Whitman, R. V. (1985). "Overburden Correction Factors for SPT in Sand", JGED, ASCE, Vol. 112, No. 3, pp. 373-377.
[25] Tokimatsu, K. and Seed, H. B. (1988). "Evaluation of Settlements in Sands Due to Earthquake Shaking", JGED, ASCE, Vol. 113, No. 8, pp. 861-878.
[26] Seed, H. B. and Idriss, I. M. (1982). "Ground Motions and Soil Liquefaction During Earthquakes", EERI Monograph, Earthquake Engineering Research Institute.
[27] Seed, H. B., Idriss, I. M., Makdisi, F. and Banerjee, N. (1975). "Representation of Irregular Stress Time Histories by Equivalent Uniform Stress Series in Liquefaction Analyses", Rept. No. UCB/EERC-75/29, Univ. of California, Berkeley.
[28] Harder, L. F. (1988). "Use of Penetration Tests to Determine the Cyclic Loading Resistance of Gravelly Soils During Earthquake Shaking", Ph.D. Thesis, Dept. of Civil Engin., Univ. of California, Berkeley.
[29] Seed, H. B. (1983). "Earthquake-Resistant Design of Earth Dams", Proc., Symposium on Seismic Design of Embankments and Caverns, ASCE, Philadelphia, May 6-10.
[30] Tokimatsu, K. and Yoshimi, Y. (1983). "Empirical Correlation of Soil Liquefaction Based on SPT N-Value and Fines Content", Soils and Foundations, JSSMFE, Vol. 23, No. 4, pp. 56-74.
[31] Evans, M. D. (1987). "Undrained Cyclic Triaxial Testing of Gravels - The Effect of Membrane Compliance", Ph.D. Thesis, Dept. of Civil Engin., Univ. of California, Berkeley.
[32] Hynes, M. E. (1988). "Pore Pressure Generation Characteristics of Gravel Under Undrained Cyclic Loading", Ph.D. Thesis, Dept. of Civil Engin., Univ. of California, Berkeley.
[33] Marcuson, W. F. and Hynes, M. E. (1990). "Stability of Slopes and Embankments During Earthquakes", Proc., ASCE/Penn. DOT Geotechnical Seminar, Hershey, Penn., April 10-11.
[34] Casagrande, A. (1936). "Characteristics of Cohesionless Soils Affecting the Stability of Slopes and Earth Fills", J. of Boston Soc. of Civil Engrs.
[35] Schofield, A. and Wroth, C. P. (1968). "Critical State Soil Mechanics", McGraw-Hill, London.
[36] Poulos, S. J., Castro, G. and France, W. (1985). "Liquefaction Evaluation Procedure", JGED, ASCE, Vol. 111, No. 6, pp. 772-792.
[37] Seed, H. B. (1986). "Design Problems in Soil Liquefaction", JGED, ASCE, Vol. 113, No. 8, pp. 827-845.
[38] Bennett, M. J. (1989). "Liquefaction Analysis of the 1971 Ground Failure at the San Fernando Valley Juvenile Hall, California," Bull. of the Assoc. of Engin. Geologists, May.

[39] Bryant, S. M., Duncan, J. M. and Seed, H. B. (1983). "Application of Tailings Dam Flow Analyses to Field Conditions," Report No. UCB/GT/83-03, Dept. of Civil Engin., University of California, Berkeley, California.
[40] Davis, A. P., Castro, G. and Poulos, S. J. "Strengths Backfigured from Liquefaction Case Histories", Proc., Second Int'l. Conf. on Case Histories in Geotechnical Eng'g., Missouri, Rolla, June 1-5.
[41] De Alba, P., Seed, H. B., Retamal, E. and Seed, R. B. (1987). "Residual Strength of Sand from Dam Failures in the Chilean Earthquake of March 3, 1985", Report No. UCB/EERC-87/11, University of California, Berkeley.
[42] Harder, L. F. and Driller, M. W. (1990). "Examination of the Performance of Upper San Fernando Dam During the Earthquake of February 9, 1971", Report in progress.
[43] Ishihara, K. (1984). "Post-Earthquake Failure of a Tailings Dam Due Liquefaction of the Pond Deposit," Proc., Intl. Conf. on Case Histories in Geotechnical Eng'g., St. Louis, Mo., May 6-11, Vol. III, pp. 1129-1146.
[44] Lucia, P. C. (1981). "Review of Experience with Flow Failures of Tailings Dams and Waste Impoundments," Ph.D. Thesis, Dept. of Civil Engin., Univ. of California, Berkeley.
[45] Marcuson, W. F. III, Ballard, R. R., Jr. and Ledbetter, R. H. (1979). "Liquefaction Failure of Tailings Dams Resulting from the Near Izu Oshima Earthquake, 14 and 15 January, 1978", Proc. of the 6th Pan-American Conf. on Soil Mech. and Found. Engin., Lima, Peru.
[46] Ross, G. A. (1968). "Case Studies of Soil Stability Problems Resulting from Earthquakes", Ph.D. Thesis, Dept. of Civil Engineering, University of California, Berkeley.
[47] Ross, G. A., Seed, H. B. and Migliaccio, R. R. (1969). "Bridge Foundations in Alaska Earthquake", Journal of the Soil Mechanics and Foundations Division, ASCE, Vol. 95, No. SM4.
[48] Newmark, N. N. (1965). "Effects of Earthquakes on Dams and Embankments", Geotechnique, Vol. 5, No. 2, June.
[49] Makdisi, F. I. and Seed, H. B. (1977). "A Simplified Procedure for Estimating Earthquake-Induced Deformations in Dams and Embankments", Rept. No. UCB/EERC-77/19, University of California, Berkeley.
[50] Seed, H. B. and Makdisi, F. I. (1978). "Simplified Procedure for Estimating Dam and Embankment Earthquake-Induced Deformations", JGED, ASCE, Vol. 104, No. GT7, pp. 967-994.

18

Dynamic Loading Effects on Pile Capacities

*Robert G. Bea**

INTRODUCTION

Pile foundations for offshore platforms have been designed conventionally using static or pseudo-static methods. Loadings have been generally treated as static. Dynamic cyclic loading effects have been explicitly addressed in pile lateral soil resistance characterizations through "cyclic P-Y" (lateral load-displacement) curves. However, such effects have not been explicitly addressed in definition of axial soil resistance characteristics. Static, pile capacity methods have been used to determine the pile penetrations for the foundations of the more than 6,000 offshore platforms that are now located on the world's continental shelves. These foundations have had a remarkably good record of reliability.

Recently, the offshore industry has begun development of a new generation of deep water platforms in which dynamic loadings developed by storm waves, and in some cases, earthquakes, are of critical importance. Some of these structures are floating buoyant platforms in which very large tensile forces are transmitted to the pile foundations. Given storms or earthquakes, dynamic cyclic forces are superimposed on these tensile loadings, and there is concern for "cyclic creep pull-out" of the piles.

Some of the new generation of deep water, bottom-founded structures are being designed so that dynamic cyclic loadings are an unusually large proportion of the total design loading for the

*Robert Bea is a professor of Civil Engineering and Naval Architecture & Offshore Engineering at the University of California, Berkeley, Berkeley, CA 94720.